

Department of Neuroscience

Uppsala University

Research group Formation and Function of Neuronal Circuits

(Head: Professor Klas Kullander)

**Loss of the neuronal nuclear protein in oriens lacunosum
moleculare interneurons in the ventral hippocampus of mice**

Bachelor's thesis

University of Veterinary Medicine Vienna

Submitted by

Claudia Amort

Vienna, May 2021

External supervisors:

Prof. Klas Kullander

Angelica Thulin

Internal supervisor:

Dipl.-Biol. Dr.rer.nat. Rudolf Moldzio

Reviewer:

Ao.Univ.-Prof. Dr.med.vet. Alois Strasser

Table of contents

1. Introduction.....	1
1.1 Memory encoding	1
1.2 The indirect and direct pathways to the hippocampus	1
1.3 Memory consolidation.....	3
1.4 OLMa2 cells	3
1.5 The function of OLMa2 cells	3
1.6 The regulators of OLM cells.....	4
1.7 The role of OLM cells in behavior.....	5
1.8 Loss of the neuronal nuclear protein	6
2. Aim	8
3. Materials and Methods	9
3.1 Mouse strains	10
3.2 Virus	10
3.3 Perfusion.....	10
3.4 Creation of sections: Vibratome - mice A, C, D, E.....	11
3.5 Creation of sections: Cryostat - mice B, F.....	11
3.6 Immunohistochemistry: Floating sections - mice A, C, D, E, F.....	11
3.6.1 Protocol 1 - mouse A.....	11
3.6.2 Protocol 2 - mice C, D, E, F	12
3.7 Immunohistochemistry: Sections on a glass slide - mouse B.....	12
3.8 Image acquisition and analysis	13
3.8.1 Comparison of methods to create sections.....	13
3.8.2 Observation of the virus spread	14
3.8.3 Observation of the downregulation of NeuN.....	15
3.8.4 Properties for the observation of the remaining figures	17
4. Results	18
4.1 Establishment of the method to create sections: mice A, B	18

4.2 Observation of the virus spread: C, D, E, F.....	22
4.3 Loss of NeuN in OLM α 2 cells.....	27
5. Discussion	29
5.1 Significance of NeuN	29
5.2 Detection of NeuN in OLM α 2 cells	29
5.3 Correlation between the NeuN expression and the age of mice	30
5.4 Loss of NeuN in OLM α 2 cells.....	30
5.5 Spread of the virus in the brain.....	31
5.6 Imaging.....	32
5.7 Ethical discussion.....	32
5.8 Outlook on future projects	33
5.9 Conclusion	33
6. Summary	35
7. Zusammenfassung.....	36
8. Keywords and abbreviations	37
9. Contributions	39
10. Acknowledgments	40
11. References.....	41
12. Appendix.....	47
12.1. Mouse strains	47
12.1.1 Chrna2-cre/tdTomato	47
12.1.2 Chrna2-cre/Cas9EGFP	47
12.1.3 Genotyping	47
12.2. Virus	49
12.2.1 Virus production.....	49
12.2.2 Virus injection: mice C, D, E, F.....	49
12.3. Perfusion	50

1. Introduction

The brain has a remarkable capacity to collect new information from the environment, to store it, and to adapt the behavior accordingly (Daoudal and Debanne 2003). The hippocampus plays an important role in this task, especially for memory formation, navigation through space, the experience of time, and it is also closely tied to emotional processing. In the human brain, the hippocampus is an elongated structure in the temporal lobe. The posterior hippocampus, equivalent to the dorsal part in rodents, receives spatial and visual input and is essential for cognitive functions. The anterior, in rodents ventral, part receives olfactory information, is associated with limbic structures, and hence correlates with stress and emotion (Fanselow and Dong 2010; Strange et al. 2014).

1.1 Memory encoding

Memory formation is a complex process that occurs in the hippocampus and cortex. In the initial learning of information, a process called memory encoding occurs. Perceived events like sensory inputs are converted and can be stored for a shorter or longer term. The information gets transferred through the entorhinal cortex (EC) to the hippocampus either by accessing the perforant or the temporoammonic pathways (Doller and Weight 1982; Maccaferri and McBain 1995; Haam et al. 2018; Leão et al. 2012). In mice, it was shown that memory encoding and consolidation are temporally separated in the brain, which is important since the same cells are involved in those two pathways. They do not interfere with each other, because they are under the control of acetylcholine. This neurotransmitter is acting through specific interneurons and can suppress memory consolidation by inhibiting the output from the hippocampus and stimulating the memory encoding process (Haam et al. 2018).

1.2 The indirect and direct pathways to the hippocampus

Excitatory signals are led through the hippocampus in the trisynaptic path. Neuronal activity that enters has principal neurons involved, which are granule cells of the dentate gyrus and pyramidal cells of the cornu ammonis area 1 and 3 (CA1 and CA3). The pathway starts with axons of superficial layers of the EC that are projecting via the perforant path to dentate granule cells. Their axons form the mossy fibers and excite CA3 pyramidal cells and hilar

interneurons. CA3 pyramidal cells project to CA1 pyramidal cells with Schaffer collateral fibers. Later on, CA1 pyramidal cells can send fibers to the subiculum, EC, and other cortical areas (Knowles 1992; Alkadhi 2019; Haam et al. 2018). This intrahippocampal indirect pathway is targeting the proximal dendrites of pyramidal cells and is considered to be important for the connection of information and pattern separation as well as completion (Andersen et al. 2007; Lisman and Otmakhova 2001). From the superficial layers of the EC, projections also go directly to the CA1 via the temporoammonic pathway (Maccaferri and McBain 1995). While targeting the distal dendrites of pyramidal cells, the direct pathway is primarily responsible for recognizing if an event or context is novel (Andersen et al. 2007; Lisman and Otmakhova 2001) (Figure 1).

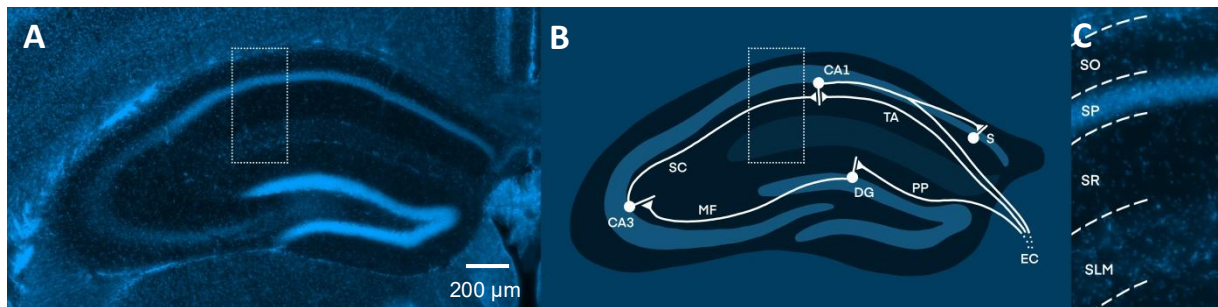


Figure 1: Pathways of the hippocampus

The figure shows a coronal section of the dorsal hippocampus. The white boxes in A and B indicate the magnified area in C. The microphotographs A and C are visualized with the help of an immunostaining targeting the neuronal nuclear protein (NeuN) with the fluorescent protein Alexa Fluor 647 (blue). B shows an illustration of A to summarize the pathways of the hippocampus. Inputs to the hippocampus come from the entorhinal cortex (EC) by the perforant path (PP) or the temporoammonic pathway (TA). The PP accesses dentate gyrus (DG) cells, which form the mossy fibers (MF), lead to cornu ammonis area 3 (CA3) pyramidal cells. These then send the Schaffer collateral (SC) fibers to cornu ammonis area 1 (CA1) pyramidal cells. They can then project to the subiculum (S), back to the EC or other cortical areas. The TP on the other hand leads from the EC to CA1 pyramidal cells. In image C, layers of the hippocampus are visible including the stratum oriens (SO), the stratum pyramidale (SP), the stratum radiatum (SR), and the stratum lacunosum moleculare (SLM). Microphotograph A was obtained in a widefield microscope with an objective of 20x (numerical aperture (NA) = 0.8) and the tiles and z-stack option.

1.3 Memory consolidation

In the hippocampus, information can be stored temporarily. During memory consolidation, the information has to be relayed to the neocortex for long-term storage. Outputs of the hippocampus reach the deep layers of the EC and then project to the neocortex. From deep layers of the EC, projections also run back to the superficial layers to complete the hippocampus–entorhinal cortical circuit (Kloosterman et al. 2003).

1.4 OLM α 2 cells

In the hippocampus, a diverse population of cell types are interneurons, they control input and output activity differently depending on their postsynaptic domains (Freund and Buzsáki 1996). To control the input and distribution of excitatory signaling in neural circuits, a negative feedback mechanism is crucial (Haam et al. 2018). One such major regulator is the oriens lacunosum moleculare (OLM) interneuron, which is a γ -aminobutyric acid (GABA)-ergic interneuron with its soma located in the outermost layer of the hippocampus, the stratum oriens (Figure 1). A genetically defined population in the CA1 layer are the OLM α 2 cells, which are OLM cells that express the neuronal acetylcholine receptor subunit alpha-2 (Chrna2) in nicotinic acetylcholine receptors (nAChR). nAChRs are ligand-gated ion channels and can activate these cells (Son and Winzer-Serhan 2008). In the hippocampus, the expression of the specific molecular marker Chrna2 is restricted to CA1 and subiculum interneurons. These cells are present in a higher number in the ventral region compared to the dorsal region. Apart from α 2, OLM cells also express other nicotinic receptor subunits like α 7 (Leão et al. 2012). Interneurons that express Chrna2 in the hippocampus also express α 4 and β 2 (unpublished analysis of RNA transcriptome data (Harris et al. 2018) from the Kullander lab at Uppsala University). Therefore, the activation of OLM cells in an ionotropic cholinergic manner is probably mediated by the α 2, α 4, and β 2 subunits.

1.5 The function of OLM α 2 cells

OLM α 2 cells are among others targeting distal apical dendritic domains of pyramidal neurons in the innermost layer, the stratum lacunosum-moleculare (Figure 1), and can modulate their cell input. In this area, the pyramidal cells also receive direct inputs coming from the EC via

the temporoammonic pathway (Leão et al. 2012; Klausberger and Somogyi 2008). When stimulating OLM α 2 cells in brain slices from mice, they decrease the probability of long-term potentiation (LTP) from the temporoammonic pathway, since therefore increased inputs would be necessary. The OLM α 2 cells gate the input signal and can thus affect LTP. In contrast, OLM α 2 cells facilitate LTP in the Schaffer collateral pathway, which is part of the trisynaptic pathway. In other words, through activation of OLM α 2 cells, they are prioritizing inputs from the indirect trisynaptic pathway over those from the direct temporoammonic pathway. A study showed that such promotion is similar to the effects of nicotine (Leão et al. 2012). Nicotine is an agonist of nAChR and it has been shown to induce inhibition, which increases the background noise due to a combined depolarization of interneurons. It also masks small phasic inhibitions from interneurons in the stratum radiatum, that do not contain the Chrna2 nAChR and that would act on specific membrane domains of pyramidal cells. This is due to ongoing inhibitory synaptic activity by nicotine (Jia et al. 2009). OLM α 2 cells could also account for the impacts of nicotine on synaptic plasticity including the memory-enhancing effects of nicotine observed *in vitro* (Leão et al. 2012; Davis and Gould 2008). Although, in an object recognition test, a relatively high dose of 1.5 mg/kg nicotine was applied, and then nicotine impaired the memory performance of mice (Siwani 2021).

OLM cells modulate direct inputs coming from the EC and internal inputs originating from CA3. On the cellular level, one of the main signals regulating LTP is Calcium²⁺ (Ca²⁺). Its concentration can be locally modulated in the dendritic compartments of the pyramidal cells. Inhibition at the distal dendrites can be enabled by closing voltage-gated Ca²⁺ channels resulting in a reduced Ca²⁺ level. With the opposite mechanism, disinhibition and rise of Ca²⁺ concentrations can be achieved at the proximal dendrites (Lynch 2004).

1.6 The regulators of OLM cells

A study in mice showed that OLM cells themselves, like other GABAergic cells in the CA1 area of the hippocampus, are targeted by calretinin- and/or vasoactive intestinal polypeptide-expressing interneuron-specific cells. These cells can be further subdivided into three subtypes. The type 3 interneuron-specific cells are located in the stratum pyramidale or radiatum (Figure 1) and preferably contact metabotropic glutamate receptor 1a-positive OLM

cells. Their efficiency of transmission at the synapse is relatively weak, but many cells can synchronously generate a spike and target a single postsynaptic cell. Therefore, interneuron-specific cells can control the firing rate and timing of OLM interneurons. In conclusion, dendritic inhibition from interneuron-specific cells is needed for the feedback inhibition of OLM interneurons (Tyan et al. 2014).

Inputs from outside the hippocampus that target OLM cells are mainly coming from the medial septum (Haam et al. 2018). These inputs can be cholinergic (Lawrence et al. 2006), but also GABAergic and glutamatergic projections are present, although for these two it is less known about their specific connection to OLM α 2 cells (Whittington et al. 1995). Inputs from the medial septum can lead to an excitation of OLM cells and then, they can suppress LTP in the temporoammonic pathway (Leão et al. 2012), explicitly the excitatory connections in the CA3 region of the hippocampus get depotentiated. Then inputs coming from the CA3 region are strong and this allows the retrieval and also unlearning of old information. When on the other hand, new inputs coming from the EC are strong and LTP of excitatory connections in the CA3 is strong as well, novel associations are able to be encoded. Then the transmission at these synapses is weak, and consequently, old patterns are not able to interfere (Hasselmo, Bodelón, and Wyble 2002).

1.7 The role of OLM cells in behavior

As the hippocampus is functionally segregated along the dorsoventral axis is it possible that also OLM cells play different roles in the dorsal and ventral part (Haam et al. 2018; Fanselow and Dong 2010). Related to fear learning, two studies in mice were conducted that support this claim. A first study showed that inactivation in the dorsal hippocampus of somatostatin positive cells, like OLM cells prevents fear-related learning (Lovett-Barron et al. 2014). A second study in intermediate OLM α 2 cells revealed that decreased learning was achieved upon acute activation, not inhibition (Siwani et al. 2018). Consistently with these findings, also nicotine has opposite effects in the dorsal and ventral hippocampus. When providing nicotine to the dorsal hippocampus, it enhances memory associated with contextual fear. On the other hand, whereas administering it in the ventral part, it impairs it (Kenney, Raybuck, and Gould 2012). When stimulating ventral OLM α 2 cells, increased risk-taking behavior was

observed in response to predator odor, which is anxiogenic (Mikulovic et al. 2018). These results suggest that the hippocampus plays an important role in defensive behaviors and emotional processing during threatening events.

1.8 Loss of the neuronal nuclear protein

In this study, the neuronal nuclear (NeuN) protein is the target for detecting its loss after the knockout of the corresponding gene. NeuN is abundantly expressed in most neurons in the brain including the *Chrna2* expressing cells and hence a good control for a gene knockout (Gusel'nikova and Korzhevskiy 2015; Cannon and Greenamyre 2009). This protein has a turnover of approximately five days (Fornasiero et al. 2018). It is located in nuclei and the perinuclear cytoplasm (Gusel'nikova and Korzhevskiy 2015; Cannon and Greenamyre 2009) and is believed to be a regulatory molecule that acts on the level of the nucleus (Mullen, Buck, and Smith 1992). As it is associated with the nucleus, the detection of NeuN is independent of the volume of the cytoplasm and can even be detected in small neurons with little cytoplasm in their soma (Kim, Adelstein, and Kawamoto 2009; Kim et al. 2013). It has been shown that the NeuN protein is a Fox-3 gene product, which is part of the Fox-1 gene family of splicing factors (Kim, Adelstein, and Kawamoto 2009). A possibility to lower the concentration levels of a protein is to target it by the Clustered Regularly Interspaced Short Palindromic Repeats (CRISPR)/Cas9 gene-editing technology (Cong et al. 2013). This can insert mutations into the gene of interest, knock it out, and therefore downregulate the encoded protein (Peng et al. 2019). A transgenic mouse strain expressing the cre recombinase under the control of the *Chrna2* promoter (Leão et al. 2012) can be used, when crossed with a strain that encodes for the endonuclease Cas9 in a cre-dependent manner (Cortez et al. 2020; Platt et al. 2014). After delivering small guide RNA (sgRNA) sequences with an adeno-associated virus (AAV), it enables a region-specific gene editing in neurons expressing the *Chrna2* (Peng et al. 2019).

This study was conducted to begin to investigate the significance of OLM α 2 cells and the importance of cholinergic activation in their regulation. In humans, mutations in the *Chrna2* gene could be connected to epilepsy (Aridon et al. 2006) and benign familial infantile seizures

(Trivisano et al. 2015). This shows that basic science is needed to understand the cause of neuronal diseases and to possibly find a treatment.

2. Aim

OLM α 2 cells are interneurons that are activated by nAChRs and contain the α 2 subunit. These are among others targeting pyramidal neurons, which are involved in pathways of the hippocampus. So following questions arise: What regulatory significance do OLM α 2 have in these circuits? What effect would a disinhibition of these cells have on a cellular and behavioral level? These questions can be addressed by conducting a study in transgenic mice where the *Chrna2* subunit is downregulated and observations of the resulting effects are made. A possibility to lower the protein level is by using a CRISPR/Cas9 system to create a mutation in the gene corresponding to the protein.

To see if such a knockout would work, my thesis was conducted with a transgenic mouse strain crossbreed that genetically encodes for the Cas9 and enhanced green fluorescent protein (EGFP) in cells expressing the α 2 subunit. In the OLM α 2 cells, not the *Chrna2*, but the NeuN protein was targeted. This is abundantly expressed in most neurons in the brain including the *Chrna2* expressing cells and should hence be a good control of downregulation. In this study, we used an AAV delivering sgRNA to target the gene which encodes for the NeuN in a mouse strain, that produces the endonuclease Cas9 only in the *Chrna2* positive cells.

The following questions should be answered in this work:

Which methods to prepare the tissues are providing the best results for the analysis?

Is the NeuN indeed abundantly expressed in all OLM α 2 cells?

What injection volume of the virus allows a spread to the targeted area?

Is the Cas9 protein functional in this setup?

3. Materials and Methods

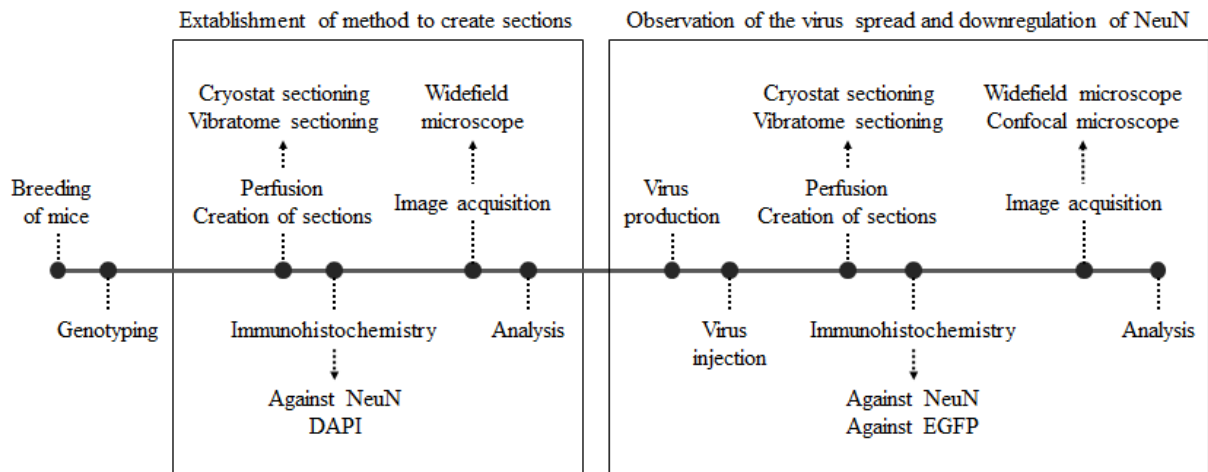


Figure 2: Workflow scheme describing how the project was organized.

This figure shows a timeline of all the procedures that were performed for this project.

Table 1: Library of the mice that were part of this project.

ID	Method to create the sections	Purpose
A	Vibratome	comparison of methods to create sections
B	Cryostat	comparison of methods to create sections
C	Vibratome	observation of the virus spread: 250 nl and downregulation of NeuN
D	Vibratome	observation of the virus spread: 500 nl and downregulation of NeuN
E	Vibratome	observation of the virus spread: 750 nl and downregulation of NeuN
F	Cryostat	observation of the virus spread: 500 nl and downregulation of NeuN

Every mouse was assigned an identification (ID) and in this table identified with the method to create the sections and their purpose.

3.1 Mouse strains

The animal experiments used in this study were approved by the local Swedish ethical committee (Dnr C63/16). All animals were kept, bred, and housed according to the regulation and guidelines of Jordbruksverket with the ethical permission (Dnr 5.8.18-11551/2019). Two transgenic mouse strain crossbreeds were used, where one is expressing the cre recombinase under the control of the *Chrna2* promoter (Leão et al. 2012) and a genetic construct for the tdTomato fluorescent protein (JAX stock #007914; Madisen et al. 2010). The other mouse strain crossbreed is also expressing the cre recombinase under the control of the *Chrna2* promoter, but with the Cas9 and EGFP protein (JAX stock #026179; Cortez et al. 2020; Platt et al. 2014) in a cre-dependent manner.

3.2 Virus

An AAV was used, which delivered sgRNA sequences to confirm the function of Cas9 when targeting the *Rbfox3* gene (encodes the NeuN protein) at a titer of 2.70×10^{12} viral genome (VG)/ml. The mice C, D, E, and F were injected unilaterally with the virus intracerebrally. Two mice were injected with a volume of 500 nl, one with 250 nl, and one with 750 nl.

3.3 Perfusion

To prepare the tissue for immunohistochemistry, the brains were fixed by transcardial perfusions. The two *Chrna2-cre/tdTomato* mice were sacrificed and perfused after eight weeks of age. The perfusion for mouse D was performed nine days after injecting the virus and mice C, E, F were perfused after 24 days. When sacrificed, mice D and F were 36 weeks and the other two 29 weeks old.

For my thesis, I used fixed brains provided by colleagues from the Kullander group: Formation and Function of Neuronal Circuits of the Department of Neuroscience at the Uppsala University, Uppsala, Sweden. More information about the methods that allowed me to do my experiments can be found in the Appendix.

3.4 Creation of sections: Vibratome - mice A, C, D, E

The brain was placed in 4 % agarose in 1× phosphate buffered saline (PBS) and then cut in coronal sections using the vibratome (Leica VT 1000S Vibrating blade microtome, Leica Biosystems Division of Leica Microsystems Inc., USA) while the tissue was submerged in 1× PBS. The frequency was set at 7 and the thickness 60 nm. The sections were saved in a well plate with 1× PBS and stored at 4 °C for the immunohistochemistry and analysis of the sections.

3.5 Creation of sections: Cryostat - mice B, F

The brain was embedded in cryostat embedding medium (Killik, Bio-Optica, Italy) in a mold and placed on dry ice to harden. The tissue for the comparison was cut at 35 nm in coronal sections with the cryostat (Leica® Reichert Jung® Cryocut 1800 Cryostat, Mercedes Scientific, USA). Then it was mounted directly on glass slides (Epredia™ SuperFrost Plus™ Adhäsionsobjektträger, Thermo Fisher Scientific Inc., USA) and stored at -80 °C until use. The brain of mouse F was cut at 40 nm in coronal sections. In an alternating matter, the sections were mounted directly on glass slides or put in a well plate with 1× PBS. The glass slides were placed at -80 °C and the well plate at 4 °C.

3.6 Immunohistochemistry: Floating sections - mice A, C, D, E, F

3.6.1 Protocol 1 - mouse A

To visualize the targeted proteins, an immunohistochemistry was performed with fluorescent proteins associated with antibodies. First, the well plate was washed 2× 10 min in 1× PBS. It was incubated at room temperature (~20 °C) for 1 h in supermix (0.5 % TritonX-100 (Triton™ X-100, Sigma-Aldrich Corp., USA), 0.25 % gelatin (Fisher Chemical™, UK) in 1× PBS) and then blocked for 1 h in blocking solution (5 % donkey serum, 0.1 % TritonX-100 in 1× PBS). The primary monoclonal antibody mouse anti-NeuN (EMD Millipore Corp., USA. It was protein A purified by the company.) was diluted 1:500 (from the stock concentration of 1 mg/ml) in blocking solution and the sections were incubated with 500 µl for 24 h at 4 °C. The well plate was washed 4× 10 min in 1× PBS. The secondary polyclonal

antibody Alexa Fluor 647 donkey anti-mouse (Life Technologies, USA. It was affinity-purified by the company.) was diluted 1:200 (from the stock concentration of 1 mg/ml) in blocking solution with 6.7 nmol/ml 4', 6-diamidino-2-phenylindol (DAPI) (VWR; USA). The slides were incubated with 500 μ l for 2 h at room temperature. Finally, the slides were washed 4 \times 10 min in 1 \times PBST (0.1 % Tween20 in 1x PBS) and embedded in anti-fade fluorescence mounting medium (Abcam, United Kingdom). The ends of the coverslip were sealed the next day with nail polish.

3.6.2 Protocol 2 - mice C, D, E, F

The well plate was washed 3 \times 5 min in 1 \times PBS. It was incubated at room temperature for 2 h in blocking solution (5 % goat serum, 0.1 % TritonX-100 in 1 \times PBS). The primary antibody mouse anti-NeuN was diluted 1:500 and the polyclonal chicken anti-GFP (Aves Labs, USA. It was affinity-purified by the company.) was diluted 1:1000 (from the stock concentration of 10 mg/ml) in blocking solution. Then the sections were incubated with 500 μ l for 24 h at 4 $^{\circ}$ C. The well plate was washed 3 \times 5 min in 1 \times PBS. The secondary polyclonal antibody Alexa Fluor 647 goat anti-mouse (Abcam, United Kingdom. It was immunogen affinity purified by the company) was diluted 1:200 (from the stock concentration of 2 mg/ml) and the Alexa Fluor 488 goat anti-chicken (InvitrogenTM, USA) was diluted 1:1000 in 1 \times PBST (0.1 % Tween20 in 1x PBS). The slides were incubated with 500 μ l for 2 h at room temperature. Finally, the slides were washed 3 \times 5 min in 1 \times PBS and embedded in anti-fade fluorescence mounting medium. The ends of the coverslip were sealed the next day with nail polish.

3.7 Immunohistochemistry: Sections on a glass slide - mouse B

The selected slides were thawed at room temperature for 1 h in a humid chamber and then washed 4 \times 10 min in 1 \times PBS. They were incubated at room temperature for 1 h in supermix (0.5 % TritonX-100, 0.25 % gelatin in 1 \times PBS) and then blocked for 1 h in blocking solution (5 % donkey serum, 0.1 % TritonX-100 in 1 \times PBS). The primary antibody mouse anti-NeuN was diluted 1:500 in blocking solution and the slides were incubated with 500 μ l for 24 h at 4 $^{\circ}$ C. The slides were washed 4 \times 10 min in 1 \times PBS. The secondary antibody Alexa Fluor 647 donkey anti-mouse was diluted 1:200 in blocking solution with 200 nmol/ml DAPI. The

slides were incubated with 500 μ l for 2 h at room temperature. Finally, the slides were washed 4 \times 10 min in 1 \times PBST (0.1 % Tween20 in 1x PBS) and embedded in anti-fade fluorescence mounting medium. The ends of the coverslip were sealed the next day with nail polish.

3.8 Image acquisition and analysis

3.8.1 Comparison of methods to create sections

To evaluate the brain sections, they were observed under the widefield microscope (Axio Imager.Z2, Carl Zeiss Microscopy GmbH, Germany). The pictures were obtained in 10x (numerical aperture (NA) = 0.45) and 20x (NA = 0.8) magnification (Table 3 and Table 4). For all the images with the tiles modus, the method Stitching was applied in Zen blue (Carl Zeiss Microscopy GmbH, Version 3.3.89.0000). In the sections from the cryostat obtained at 10x magnification, in Zen blue, the maximum in the histogram was set at 5.000. For the areas observed at 20x magnification, multiple images were obtained at the same position with the focus in different heights of the z-axis. These were merged in Zen blue with the Extended Depth of Focus method. In Figure 4 for J, K and L, the maximum of the brightness and contrast was set to 160 in ImageJ (NIH, Version 1.53c). In Figure 5 for J, K, and L, in Zen blue the maximum in the histogram was set at 2.500 and the maximum of the brightness and contrast was set to 160 in ImageJ. The montages were created with Adobe Illustrator (Adobe, Version 25.2.2) and Image J.

Table 3: Image acquisition properties for the vibratome sections

		TdTomato (Chrna2 cells)	Alexa fluor 647 (NeuN)	DAPI
	excitation wavelength	554 nm	650 nm	350 nm
	emission wavelength	581 nm	665 nm	470 nm
	artificial color	green	blue	light blue
10x	Light source intensity	92.9 %	50.3 %	N/A
	Exposure time	800 ms	300 ms	N/A
20x	Light source intensity	42.1 %	27.2 %	23.7 %
	Exposure time	1500 ms	527 ms	480 ms

The sections cut with the vibratome were observed with these properties under the widefield microscope. The excitation and emission wavelengths are from Thermo Fisher Scientific, USA.

3.8.2 Observation of the virus spread

The brain sections were observed under the widefield microscope. The pictures were obtained in 10x magnification (NA = 0.45) with the light source intensities and exposure times stated in Table 5. For all the images the method Stitching was applied in Zen blue. The montages were then created with Adobe Illustrator (Adobe, Version 25.2.2).

Table 4: Image acquisition properties for the cryostat sections

		TdTomato (Chrna2 cells)	Alexa fluor 647 (NeuN)	DAPI
10x	Light source intensity	92.8 %	50.3 %	N/A
	Exposure time	800 ms	633 ms	N/A
20x (dorsal, intermediate)	Light source intensity	93.8 %	76.4 %	9.8 %
	Exposure time	800 ms	633 ms	400 ms
20x (ventral)	Light source intensity	42.1 %	27.2 %	23.7 %
	Exposure time	1500 ms	527 ms	480 ms

The sections cut with the cryostat were observed with these properties under the widefield microscope.

Table 5: Image acquisition properties

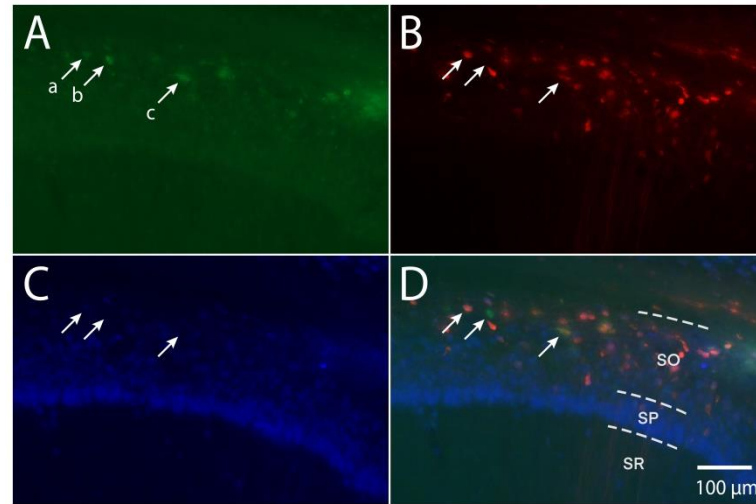
		mCherry (virus spread)	Alexa fluor 647 (NeuN)			mCherry (virus spread)	Alexa fluor 647 (NeuN)		
		excitation wavelength	587 nm	650 nm			excitation wavelength	587 nm	650 nm
		emission wavelength	610 nm	665 nm			emission wavelength	610 nm	665 nm
		artificial color	red	blue			artificial color	red	blue
mouse C	Light source intensity	10 %	20 %	mouse E	Light source intensity	15 %	25 %		
	Exposure time	50 ms	150 ms		Exposure time	50 ms	200 ms		
	Maximum in the histogram	15.000	9.000		Maximum in the histogram	11.000	5.000		
mouse D	Light source intensity	50 %	40 %	mouse F	Light source intensity	30 %	50 %		
	Exposure time	480 ms	300 ms		Exposure time	100 ms	350 ms		
	Maximum in the histogram	3.000	9.000		Maximum in the histogram	6.000	6.000		

The sections were observed with these properties under the widefield microscope at 10x magnification (NA = 0.45). The excitation and emission wavelengths are from Thermo Fisher Scientific, USA.

3.8.3 Observation of the downregulation of NeuN

For the analysis of the loss of NeuN in the OLM α 2 cells, the sections were observed under the widefield microscope at 20x (NA = 0.8) magnification. The method Extended Depth of Focus was applied in Zen blue because multiple images were obtained at the same positions with different heights of the focus in the z-axis. The montages were then created with Adobe Illustrator.

The cells of mice A, B, and D were manually counted. Not all sections that showed a virus spread, were chosen for the analysis, only those with the widest virus spread in the outermost layer of the hippocampus. The control sections underwent the same process as the samples except for the primary antibodies that were excluded from the protocol. There the sections were incubated with only PBS. An example of how the cells were counted are shown in Figure 3.



		excitation wavelength	emission wavelength	artificial color	Light source intensity	Exposure time	Maximum in the histogram
A	Alexa Fluor 488 (Chrna2 cells)	490 nm	525 nm	green	29 %	200 ms	5.000
B	mCherry (virus spread)	587 nm	610 nm	red	29.7 %	480 ms	13.000
C	Alexa Fluor 647 (NeuN)	650 nm	665 nm	blue	20 %	300 ms	15.000

Figure 3: Counting of the loss of NeuN in OLM α 2 cells

The figure shows a coronal section of the ventral hippocampus. A, B, C of the table corresponds to A, B, C of the figure, and D is a merged image. This demonstrates an example on how the cells were counted: **a**: GFP-positive, mCherry-positive, NeuN-positive; **b**: GFP-positive, mCherry-negative, NeuN-negative; **c**: GFP-positive, mCherry-positive, NeuN-negative. In the figure, the stratum oriens (SO), the stratum pyramidale (SP), and the stratum radiatum (SR) are visible. The images were obtained in a widefield microscope with an objective of 20x (NA = 0.8) with the settings stated in the table. Excitation and emission wavelengths from Thermo Fisher Scientific, USA. The method Extended Depth of Focus was applied in Zen blue and the montage was created with Adobe Illustrator.

To validate the counting and rule out faulty results, the same areas were observed in the confocal microscope (LSM 700, Carl Zeiss Microscopy GmbH, Germany). The filters were optimized to exclude any wavelengths that might be emitted by the mCherry protein. The pictures were obtained in 20x (NA = 0.8) magnification.

3.8.4 Properties for the observation of the remaining figures

The Microphotographs A and C of Figure 1 were obtained under the widefield microscope with an objective of 20x (NA = 0.8) with the settings stated in Table 3. The method Stitching and Extended Depth of Focus were applied in Zen blue. The illustration B was created in Procreate (Savage Interactive, Version 5X), as well as the Montage.

For Figure 10, the image was obtained in the widefield microscope with an objective at 10x magnification (NA = 0.45) with the tiles option. For the Alexa Fluor 647, the light source intensity was set at 50 % and the exposure time at 250 ms. The method Stitching was applied the maximum in the histogram was set at 1.000 in Zen blue. For the mCherry, the light source intensity was set at 15 % and the exposure time at 100 ms. The method Stitching was applied the maximum in the histogram was set at 4.000 in Zen blue. The montage was then created with Adobe Illustrator.

In Figure 11, image A was obtained with the widefield microscope with an objective at 10x magnification with the settings stated in Table 5, mouse D, but the light source intensity for the Alexa Fluor 647 was set at 50 %. The images B, C, D, and E were acquired with the confocal microscope an objective at 20x magnification (NA = 0.8). For the Alexa Fluor 488, the laser was set at 4.07 %, and the detector gain at 893. For the Alexa Fluor 647 the detector gain was put at 730, for the mCherry at 613 and for both, the laser was set at 2 %. In Image J the maximum of the brightness and contrast was then set at 130 and the montage was created in Adobe Illustrator.

4. Results

4.1 Establishment of the method to create sections: mice A, B

To study OLM α 2 cells, the right methods need to be determined. First, an immunohistochemistry protocol for NeuN was optimized using a Chrna2-cre mouse strain that was crossbred with tdTomato reporter mice. These express the red fluorescent tdTomato protein in Chrna2-cre-expressing cells in the hippocampus and therefore the OLM α 2 cells could clearly be visualized. After obtaining the mice brains, they could either be cut by the cryostat or the vibratome. To determine the best sectioning method for each protocol, two mouse brains were cut with either one. The sections were examined using immunohistochemistry targeting the NeuN protein, then the images were obtained with a widefield microscope. In both brains, more OLM cells in the intermediate and ventral parts of the hippocampus could be observed compared to the dorsal area. To come to these results, the tdTomato positive cells were counted in the outermost layer of the hippocampus in the two mice in each a dorsal, intermediate, and ventral section (Figure 4.1 and Figure 5.1). On average in the dorsal section were 4 OLM α 2 cells (Figure 4.1 D and Figure 5.1 D), in the intermediate 61 (Figure 4.1 E and Figure 5.1 E) and in the ventral 164 OLM α 2 cells (Figure 4.1 F and Figure 5.1 F) (Figure 6). Cutting the brains in perfect sections could be ensured with the vibratome every time. However, on the cryostat, it was a bit more difficult and one out of five sections was too damaged to use it for observations. As the size of OLM cells is around 20 μ m, also the thickness of the sections is an important factor. The vibratome allowed to cut thicker sections at 60 μ m, which means more whole cells can be found in one section. On the cryostat, on the other hand, the brains could be cut at 35 nm. After taking all these observations into consideration, cutting with the vibratome was used for three out of the four brains for the second part of the project. The immunohistochemistry in both sections showed the NeuN protein (Figure 4.2 K and Figure 5.2 K) in OLM α 2 cells (Figure 4.1 I and Figure 5.1 I).

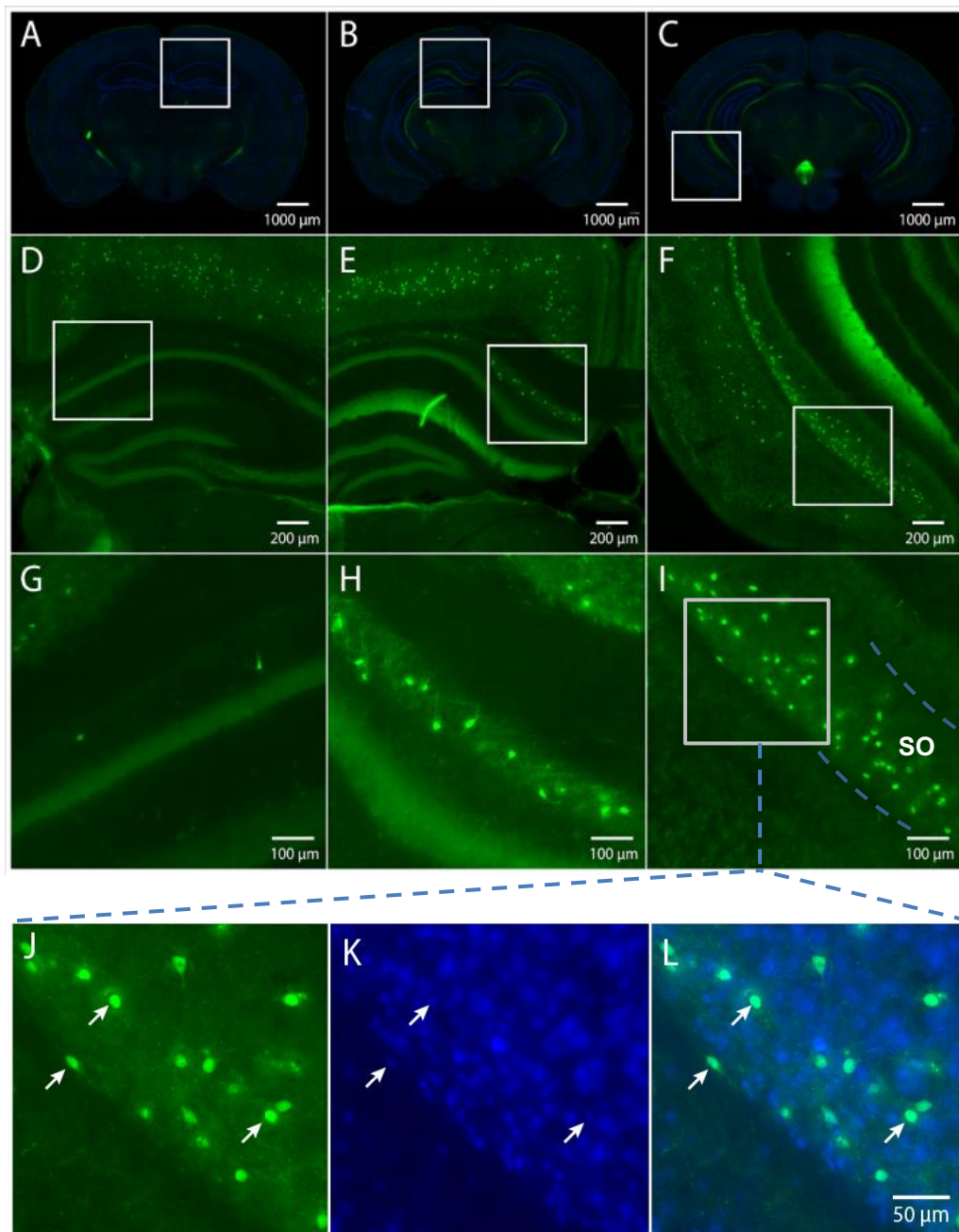


Figure 4: Observation of the brain sectioned with the vibratome

Coronal brain sections showing the hippocampus from the anterior to posterior part (A→B→C). The white boxes indicate the magnified areas (A→D→G: dorsal hippocampal area; B→E→H: intermediate hippocampal area; C→F→I→J, K, L: ventral hippocampal area). The images indicate the NeuN protein (blue) with the help of an immunostaining targeted with the fluorescent protein Alexa Fluor 647. The OLM α 2 cells (green) are visualized, due to the mouse strain that expresses the fluorescent tdTomato protein in all Chrna2 positive cells and can be found in the stratum oriens (SO) of the hippocampus (I). In the ventral hippocampus (F) more OLM α 2 cells can be found, compared to

the dorsal area (D). The last row of images shows, exemplary with at the indicated arrows, that most of the OLM α 2 cells (J) are NeuN positive (K). All images were obtained in a widefield microscope (A, B, C: objective at 10x, NA = 0.45; D, E, F, G, H, I, J, K, L: objective at 20x, NA = 0.8) with the tiles and z-stack option.

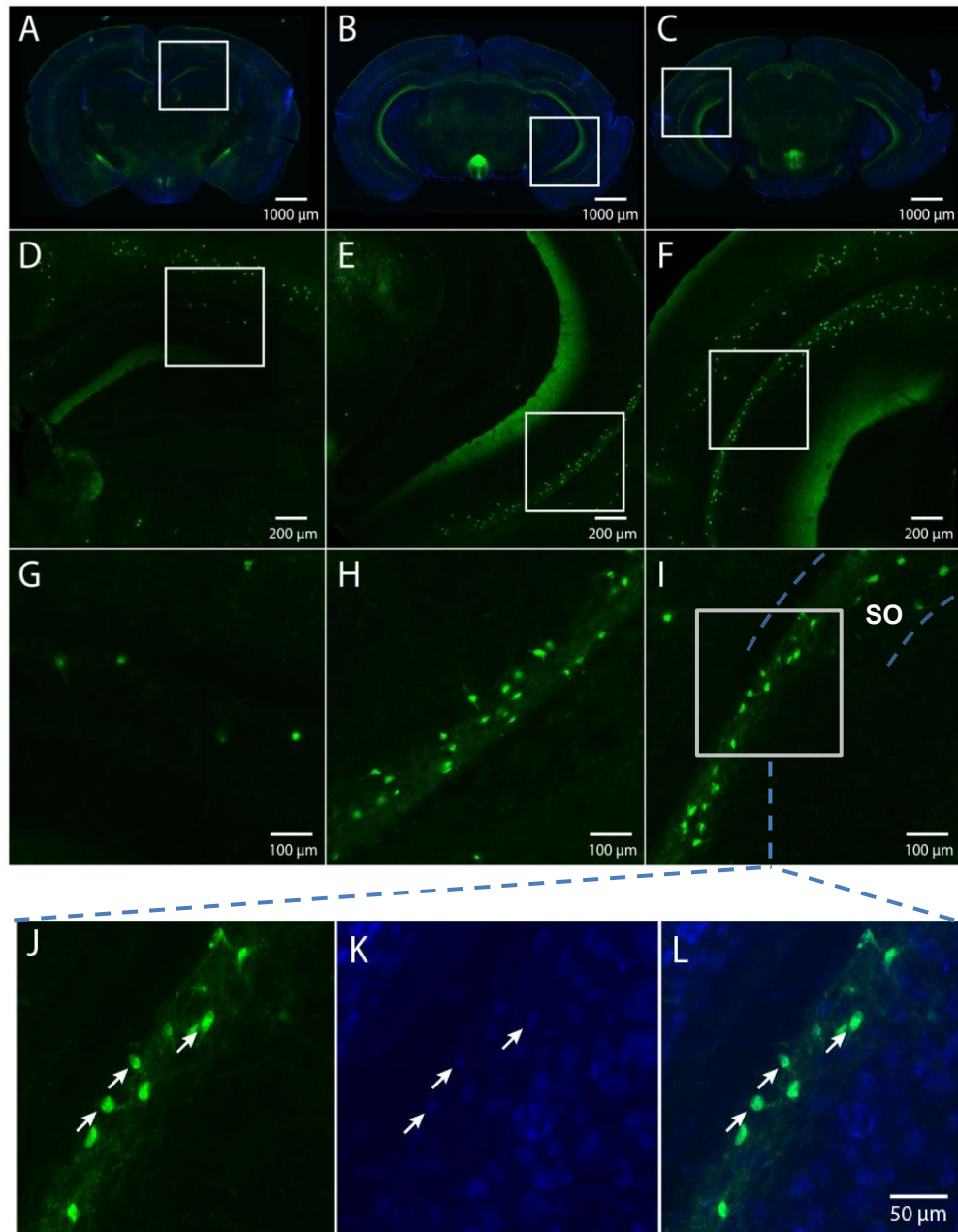


Figure 5: Observation of the brain sectioned with the cryostat

Coronal brain sections showing the hippocampus from the anterior to posterior part (A→B→C). The white boxes indicate the magnified areas (A→D→G: dorsal hippocampal area; B→E→H:

intermediate hippocampal area; C→F→I→J, K, L: ventral hippocampal area). The images indicate the NeuN protein (blue) with the help of an immunostaining targeted with the fluorescent protein Alexa Fluor 647. The OLM α 2 cells (green) are visualized, due to the mouse strain that expresses the fluorescent tdTomato protein in all Chrna2 positive cells and can be found in the stratum oriens (SO) of the hippocampus (I). In the ventral hippocampus (F) more OLM α 2 cells can be found, compared to the dorsal area (D). The last row of images shows, exemplarily with at the indicated arrows, that most of the OLM α 2 cells (J) are NeuN positive (K). All images were obtained in a widefield microscope (A, B, C: objective at 10x, NA = 0.45; D, E, F, G, H, I, J, K, L: objective at 20x, NA = 0.8) with the tiles and z-stack option.

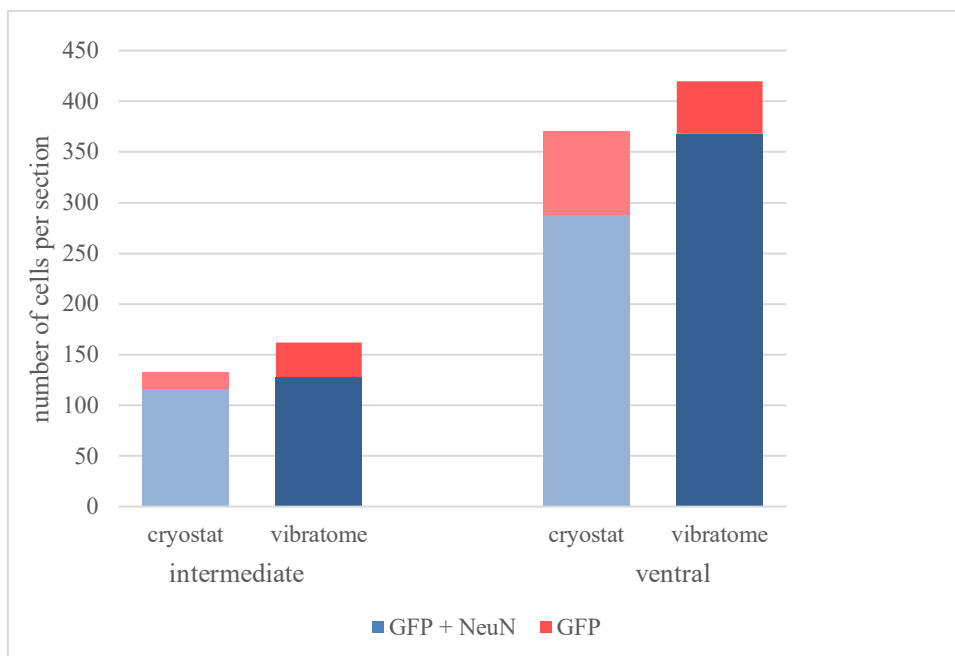


Figure 6: Comparison of the sectioning methods

The Figure shows the number of OLM cells, that could be observed in one section, when the tissue was cut with either the cryostat (lighter colors) or the vibratome (darker colors) in the intermediate and ventral areas of the hippocampus. Furthermore, it shows how many out of all the OLM cells are NeuN positive. More OLM cells could be observed in the sections cut with the vibratome and more OLM cells are in the ventral area compared to the intermediate area of the hippocampus.

4.2 Observation of the virus spread: C, D, E, F

The right injection volume is important for a successful spread to the intended area. The virus was injected into the hippocampus unilaterally with three different volumes, 250 nl, 500 nl, and 750 nl. Two mice were given a volume of 500 nl and sacrificed after nine days (Figure 8) and 24 days (Figure 10). In the first mouse, the virus couldn't spread as far as in the second mouse. The injection of 250 nl was a bit too lateral, so the virus could be found more in the cortex, rather than in the hippocampus. Nevertheless, the spread of the virus could be observed and infected an area of about 1 mm² along the transversal plane at its widest point. Also, some virus can be found in the cortex along the injection line (Figure 7). When injecting 750 nl on the other hand, the virus was capable of infecting the whole hippocampus, from ventral to dorsal (Figure 9). To detect the virus, it expressed the mCherry protein, which was especially strong in this section and caused bleed-through artifacts. The emitted light of mCherry was strong enough to be detectable when the tissue was excited with the filter range at 450-488 nm. With an amount of 500 nl, the virus could infect a wide area in the ventral hippocampus (Figure 8 and Figure 10) at an average of 2 mm² along the transversal plane at its widest point. One brain was cut with the cryostat at -20°C, but not incubated in sucrose overnight. Therefore some damage due to freezing can be observed in these sections, including many tears and tiny holes. When cut with the cryostat, the sections were mounted directly on glass slides or put in a well plate with PBS in an alternating matter to compare if one method would prevent further damages. The sections put directly into PBS were less damaged, probably because it reduced mechanical forces acting on the tissue. For example, the sections to be mounted on a glass slide had to be flattened so they could stick straight onto the glass. This was completely avoided when putting the sections directly into PBS and therefore these were used for the immunohistochemical staining. Although there are artifacts, the spread of the virus is clearly visible (Figure 10). Even though the injection was unilateral, the mCherry protein was not only observed in the injected area but also on the contralateral side in axons coming from cell bodies located in the injected area of the hippocampus. This shows interconnections between the left and right hippocampal parts. Also, the protein could be found in columns of the fornix and in the cortex. Additionally, the virus did not spread to cells in other areas of the brain, apart from the hippocampus (Figure 11).

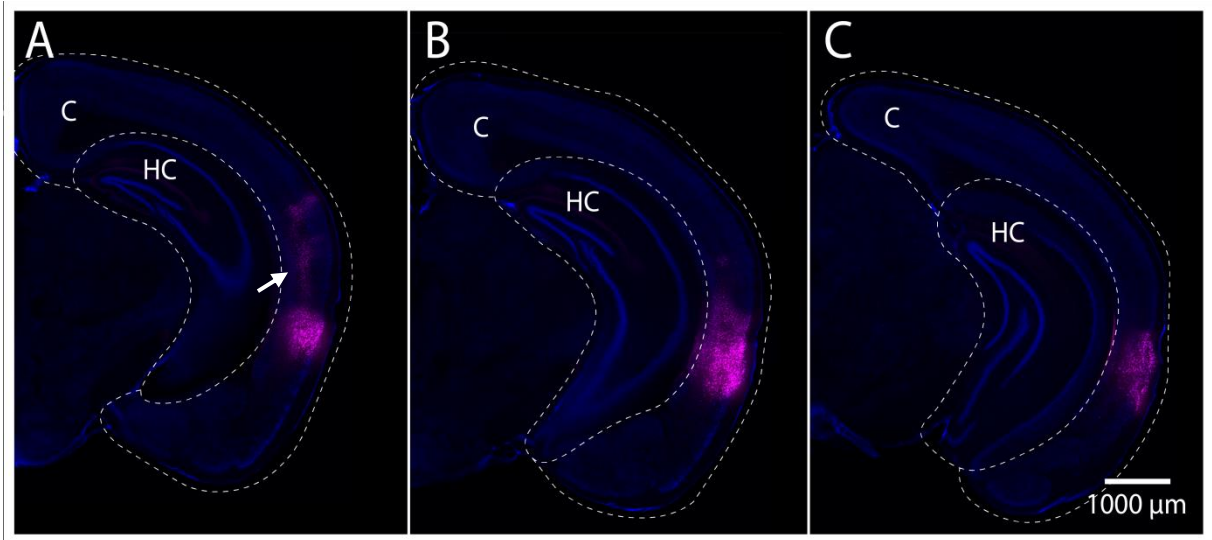


Figure 7: Observation of the virus spread after injecting 250 nl (vibratome sections)

Coronal brain sections showing half a hemisphere of the mouse brain in the dorsal (A), intermediate (B), and ventral (C) part of the hippocampus (HC). The mouse was sacrificed 24 days after the injection. The images indicate the NeuN protein (blue) with the help of an immunostaining with the fluorescent protein Alexa Fluor 647 and the injected virus (red) with the fluorescent protein mCherry. The injection was slightly off-target in the cortex (C) and spread to an area of about 1 mm^2 along the transversal plane at the widest point. Also, some virus can be found in the cortex along the injection line of the needle indicated by the arrow in A. The images were obtained in a widefield microscope with an objective at 10x magnification (NA = 0.45) with the tiles option.

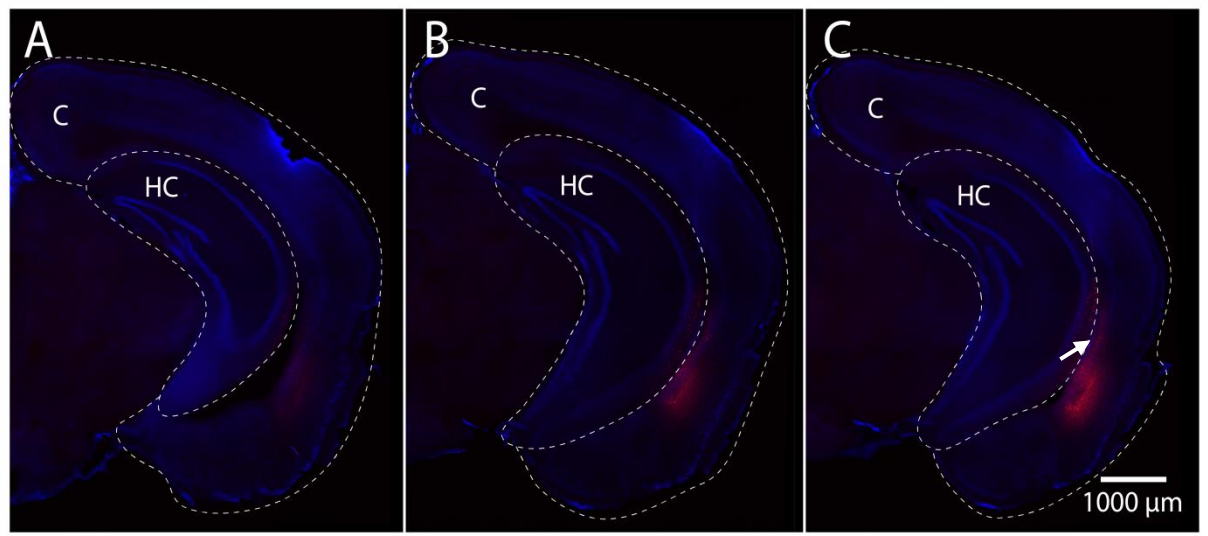


Figure 8: Observation of the virus spread after injecting 500 nl (vibratome sections)

Half a hemisphere of the mouse brain is shown in the dorsal (A), intermediate (B), and ventral (C) part of the hippocampus (HC). The mouse was sacrificed 9 days after the injection. The images indicate the NeuN protein (blue) with the help of an immunostaining targeted with the fluorescent protein Alexa Fluor 647 and the injected virus (red) with the fluorescent mCherry protein. The virus is a bit off-target in the cortex (C) more than the hippocampus since the injection was slightly too lateral or deep. Still, many OLM cells were infected and the virus infected an area of 1 mm^2 at its widest point along the transversal plane. Also, the virus can be found along the injection line in the cortex indicated by the arrow in C. The images were obtained in a widefield microscope with an objective at 10x magnification (NA = 0.45) with the tiles option.

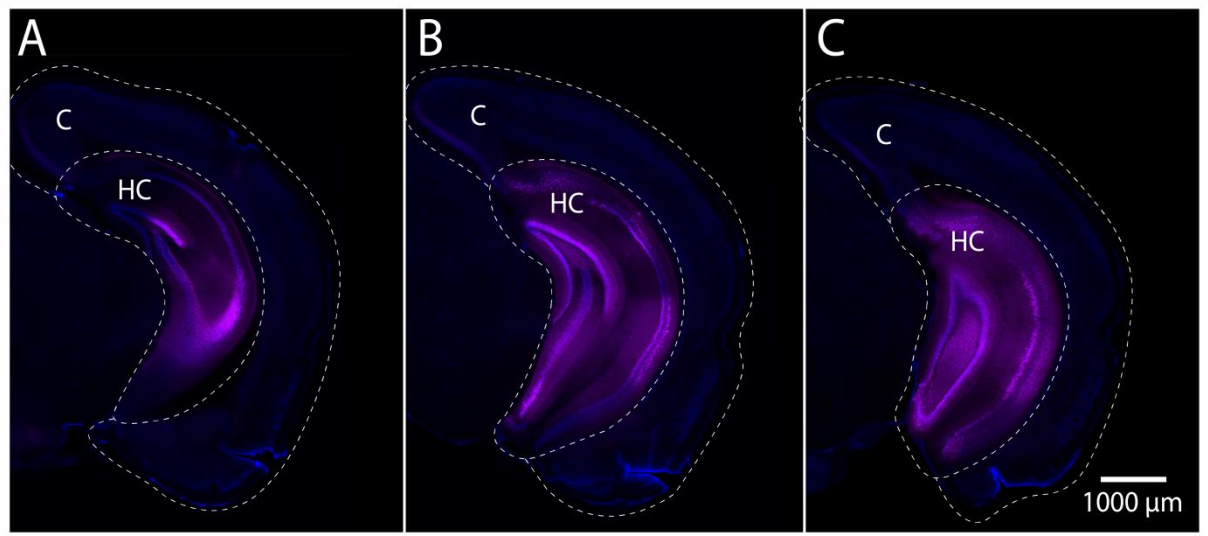


Figure 9: Observation of the virus spread after injecting 750 nl (vibratome sections)

Coronal brain sections showing half a hemisphere of the mouse brain in the dorsal (A), intermediate (B), and ventral (C) part of the hippocampus (HC). In the figure, also the cortex (C) is indicated. The mouse was sacrificed 24 days after the injection. The images show the NeuN protein (blue) with the help of an immunostaining targeted with the fluorescent protein Alexa Fluor 647 and the injected virus (red) with the fluorescent mCherry protein. With the volume of 750 nl the virus was able to infect cells all across the hippocampus from dorsal (A) to ventral (C). The images were obtained in a widefield microscope with an objective at 10x magnification (NA = 0.45) with the tiles option.

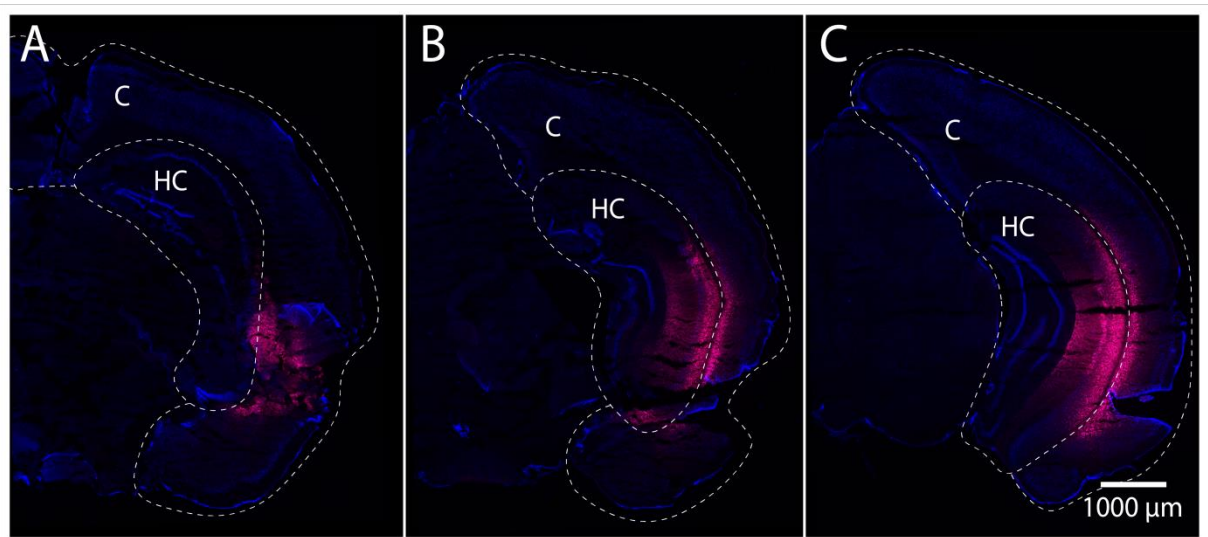


Figure 10: Observation of the virus spread after injecting 500 nl (cryostat sections)

Half a hemisphere of the mouse brain is shown in the dorsal (A), intermediate (B), and ventral (C) part of the hippocampus (HC). The mouse was sacrificed 24 days after the injection. The images indicate

the NeuN protein (blue) with the help of an immunostaining targeted with the fluorescent protein Alexa Fluor 647 and the injected virus (red) with the fluorescent mCherry protein. As the brain was not incubated in sucrose overnight, some damage due to freezing can be observed including many shutter marks and tiny holes. Although there are artifacts, the spread of the virus is clearly visible in the cortex (C), but mainly in the hippocampus. The virus could reach an area of 3 mm² at its widest point along the transversal plane and can be observed all along the dorsoventral axis, although mainly in the ventral area (C). The images were obtained in a widefield microscope with an objective at 10x magnification (NA = 0.45) with the tiles option.

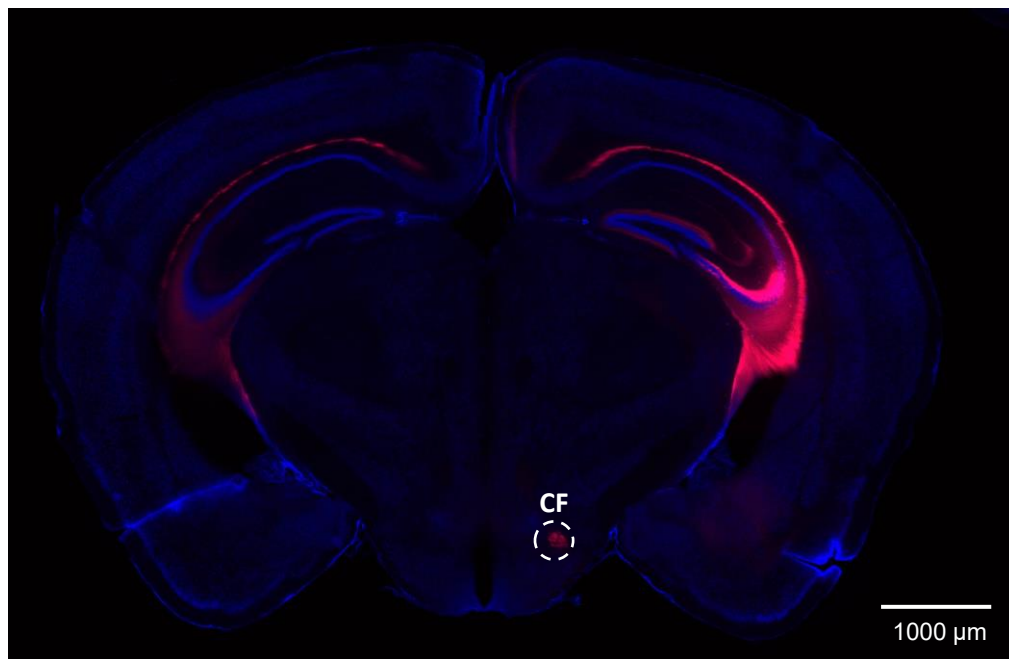


Figure 11: Observation of axonal projections originating in the virus infected area

A Coronal brain section of the hippocampus shows the axonal projections of cells that have their soma in the area, the virus was able to infect. The images indicate the NeuN protein (blue) with the help of an immunostaining targeted with the fluorescent protein Alexa Fluor 647 and the injected virus (red) with the fluorescent mCherry protein. This section of the dorsal hippocampus of the mouse with 750 nl injected, shows fluorescent fibers in the hippocampus on the contralateral side, even though the virus was injected unilaterally. Also, projections can be observed in the columns of the fornix (CF) and in the cortex. The image was obtained in a widefield microscope with an objective at 10x magnification (NA = 0.45) with the tiles option.

4.3 Loss of NeuN in OLM α 2 cells

To see if the Cas9 is functional in a *Chrna2-cre/Cas9EGFP* mouse strain crossbreed, the *Rbfox3* gene (encoding for the NeuN protein) is targeted by the sgRNA/Cas9 complex and knocked out. This lowers the NeuN protein concentrations, which can then be analyzed in coronal sections of the mouse brain. Of the four injected mice, the one with the most optimal injection and preparation was analyzed and showed loss of the NeuN protein in many cells. In this brain, the virus was able to infect an area of about 1 mm² along the transversal plane at the widest point. On nine different sections, 89 OLM α 2 cells were counted and since the virus was not able to infect cells in the ventral hippocampus on the contralateral side, 42 cells were counted of two different sections as a control. In the areas reached by the virus, 82 % of the OLM α 2 cells were infected and of these cells, about 49 % still had detectable levels of NeuN. As a comparison, in a non-virus-infected area, the expression of NeuN in 95 % of the OLM α 2 cells was detected. This mouse was 36 weeks old when sacrificed. The two mice that were part of the comparison of the methods were 8 weeks old and showed an expression of 84 % and 73 % of NeuN in the OLM α 2 cells (Figure 12 and Figure 13).

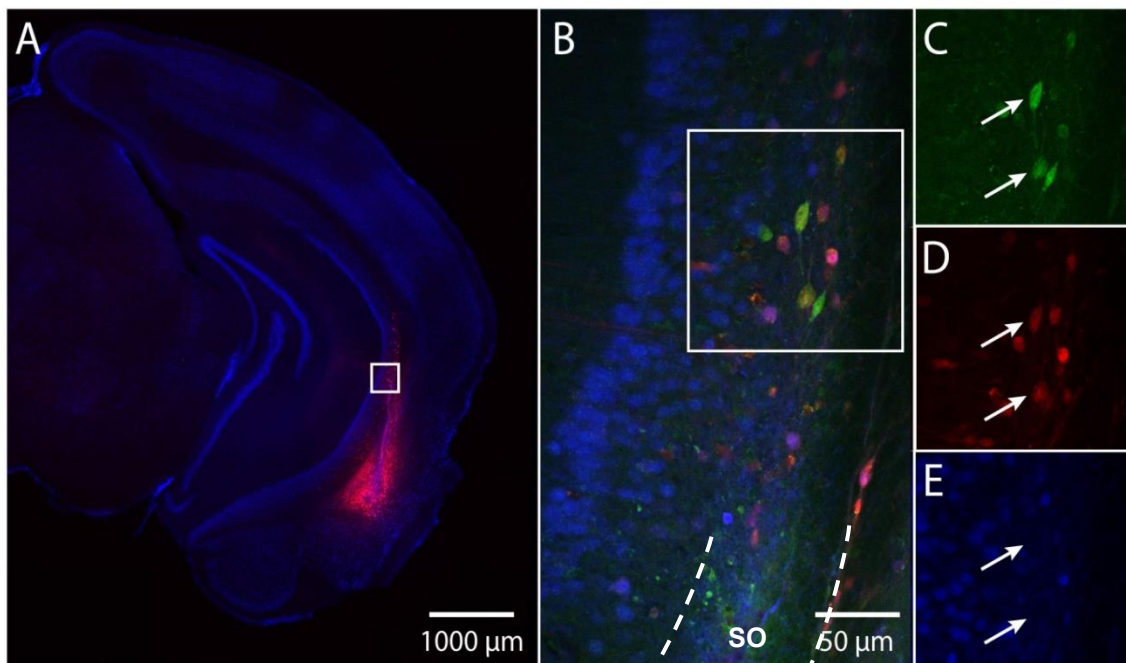


Figure 12: Observation of the loss of NeuN in OLM α 2 cells

Coronal brain section showing half the hemisphere of the mouse brain in the ventral part of the hippocampus (A). The white boxes indicate the magnified areas (A→B→C, D, E) and in B, the area

limited by the box is also the merged image of C, D, and E. The NeuN protein (blue in A, B, E) is visualized with the help of an immunostaining targeted with the fluorescent protein Alexa Fluor 647 and the virus spread (red in A, B, D) with the fluorescent mCherry protein. The OLM α 2 cells (green in B, C) can be observed due to the mouse strain that expresses the EGFP protein in all Chrna2 positive cells, which are located in the stratum oriens (SO) of the hippocampus (B). This figure shows exemplary a successful knockout of the Rbfox3 gene, which encodes for the NeuN protein. Indicated with the arrows are the OLM α 2 cells (C) which are infected with the virus (D) and have a loss of the NeuN protein (E). Image A was obtained in a widefield microscope with an objective at 10x magnification (NA = 0.45) with the tiles option. The images B, C, D, E were acquired with a confocal microscope an objective at 20x magnification (NA = 0.8).

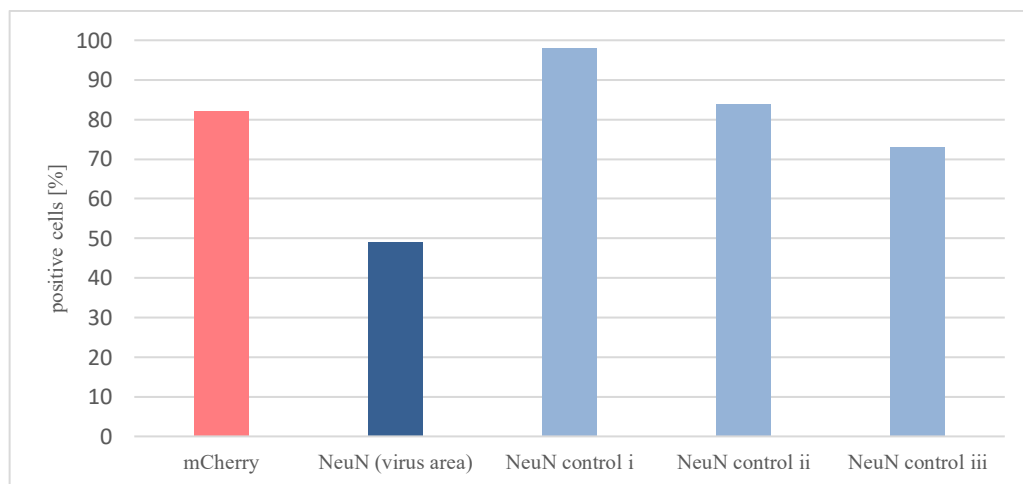


Figure 13: Loss of NeuN in OLM α 2 positive cells

The virus was able to infect 82 % of the OLM α 2 cells (mCherry). Of these cells, NeuN was lost in 49% of the cells (virus area)). In comparison, the same mouse had an expression of 95 % in a control area (control i). This mouse was 36 weeks old. Two other mice with the age of 8 weeks had an expression of 84 % (control ii) and 73 % (control iii) of NeuN in the OLM α 2 cells.

5. Discussion

In the hippocampus, OLM cells play a crucial role in the control of excitatory inputs to this structure (Haam et al. 2018). Several studies connect OLM cells to anxiety behaviors and fear-related learning (Lovett-Barron et al. 2014; Siwani et al. 2018; Mikulovic et al. 2018). These results suggest that the hippocampus plays an important role in defensive behaviors and emotional processing during threatening events.

5.1 Significance of NeuN

The neuronal population targeted in this project are OLM cells with *Chrna2* containing nicotinic receptors. The goal is to knockout these receptors using an AAV and CRISPR/Cas9 system and study that effect on behavior. First, the function of Cas9 needs to be validated in the mouse strain crossbreed. Here the target is not the *Chrna2* but the NeuN protein. This protein is abundantly expressed in most neurons in the brain including the *Chrna2* expressing cells and hence a good control of downregulation (Gusel'nikova and Korzhevskiy 2015; Cannon and Greenamyre 2009). This was also shown in the results of this project. This protein is part of a family of splicing factors (Kim, Adelstein, and Kawamoto 2009) and since alternative precursor messenger RNA (pre-mRNA) splicing is a crucial mechanism, the downregulation of the NeuN protein in neuronal cells might affect other gene products as well. Loss-of-function studies in the spinal cord revealed, that this protein is also essential for postmitotic neuronal differentiation and associated with the downregulation of general neuronal proteins (Kim, Adelstein, and Kawamoto 2009; Kim et al. 2013). If the idea was not only to confirm the function of the CRISPR/Cas9 system but also to continue with behavioral studies, the effects of NeuN on other gene products should first be investigated, to make sure the observed effects are indeed directly related to NeuN.

5.2 Detection of NeuN in OLM α 2 cells

In this project, NeuN could be observed in 84 % of the OLM cells on average, so in the majority, but not in all of the cells. This can be due to the fact that there NeuN is not expressed or at levels below the detection limit. Experimental data previously showed that there are differences, to begin with, in the immunohistochemical detection between different

neurons as well as within the same type (Gusel'nikova and Korzhevskiy 2015; Cannon and Greenamyre 2009). Furthermore, the phosphorylation of the NeuN protein has an influence on the ability to detect it. Without any phosphorylation, the epitope for the antibody binding is involved in protein-protein interactions and therefore masked. Only with at least one phosphate group, the anti-NeuN antibody can bind (Lind et al. 2005; Maxeiner et al. 2014). Also, injuries can affect the NeuN expression like axonal injury (McPhail et al. 2004) or other brain damages. After the injection of the virus, the loss of NeuN could be due to the cells dying, but a previous study showed that it is not a reliable indicator for their death (Unal-Cevik et al. 2004). Hence it is likely that the downregulation of NeuN is due to the virus and a functional CRISPR/Cas9 system. Nevertheless, this is a possible source of error and could be dismissed in future experiments by using cell death markers.

5.3 Correlation between the NeuN expression and the age of mice

The NeuN expression also changes in correspondence to the age of the animal. A study in spinal cords of rats showed a complete loss of the protein in neurons in 32-week-old animals (Portiansky et al. 2006). Surprisingly this study couldn't confirm that. The 36-week-old mouse showed a NeuN expression in 95 % of the OLM cells and in two eight-week-old mice an expression in 84 % and 73 % could be observed. It is important to note that the latter was sectioned at 40 nm and as OLM cells are on average 20 nm big, it is possible that it contained many cells, where half of the cell body was cut off. The protein to detect OLM cells is spread across the whole cell, while the NeuN protein is found associated with the nucleus. So the possibility remains, that some of these cells were counted, where the nucleus was cut off together with a lost detection of NeuN.

5.4 Loss of NeuN in OLM α 2 cells

In this pilot project, few mice were analyzed with no statistical method used. Statistics essentially turn numerical data into information to interpret it. In the case of this pilot project, the results were ready to be interpreted without applying a statistical method. Also, to confirm the function of the Cas9 protein, the observation of a tendency was sufficient. A previous study could furthermore successfully use this system in a similar setting (Peng et al. 2019). Although, in the case of using an increased number of animals and having a larger amount of

data, a statistical analysis could help understand the results. In this project the NeuN protein was lost in 49 % of the OLM α 2 cells, after the virus infected the cells. Before, the expression was at an average of 84 %. This leads to the conclusion, that the Cas9 endonuclease is functional.

5.5 Spread of the virus in the brain

Another relevant aspect is the spread of the virus. As a replication-incompetent AAV was used (Peng et al. 2019), it can only deliver its genome to the cell and can't replicate there and spread further. Meaning, that in order to study a specific area in the hippocampus, the injection amount should be chosen carefully for the optimal spread and downregulation in the intended area. As the ventral hippocampus is the main target, the virus should infect a wide area to target many OLM cells and to ensure a behavioral outcome. This was best achieved by using 500 nl at a titer of 2.70×10^{12} VG/ml. This is the optimal volume because the virus was able to infect a wide area in the ventral hippocampus, around 2 mm² at its widest point along the transversal plane. If the intention would be to target the entire hippocampus, a larger spread and hence a larger injection amount would be preferable. This could be achieved with 750 nl, then the behavioral outcome related to the whole hippocampus could be observed. As the OLM cells are likely playing different roles along the dorsoventral axis (Haam et al. 2018; Fanselow and Dong 2010), such a study could be of importance. Another observation was made when analyzing the sections of the brain. The mCherry protein, expressed by the virus could not only be found in the injected area but also on the contralateral side of the hippocampus, in the columns of the fornix and the cortex. This leads to the conclusion, that cells of the infected area are projecting to the before-mentioned structures.

The mouse strain used is a Chrna2-cre/Cas9EGFP mouse strain, which means, that all cells that express the Chrna2 subunit are able to produce the Cas9 protein. Apart from the OLM cells in the hippocampus, also Martinotti cells in layer five of the cortex are Chrna2 positive and can therefore also express the Cas9 protein (Hilscher et al. 2017). This is also true for cells in the olfactory bulb, the interpeduncular nucleus, the subiculum, the medial septum, amygdala, and others (Ishii et al. 2005). When the virus was injected, it passed the cortex and

a bit of leakage could be observed. Therefore, the chance is high, that also a few Martinotti cells were infected and downregulated the Rbfox3 gene.

5.6 Imaging

When observing the spread and loss of NeuN in the widefield microscope, bleed-through artifacts created by the mCherry could be identified, when the tissue was excited with the filter range at 450-488 nm. This is due to the mCherry molecules expressed in the cells and therefore, this protein in sum emits a lot of light. Also, the excitation curves of this protein and the Alexa Fluor 488 (excited at 450-488 nm) slightly overlap. To reduce this error, the same areas were re-examined in the confocal microscope, to better identify intracellular structures. Also, potential bleed-through could be handled by superior filters optimized to exclude any wavelengths that might be emitted by the mCherry protein. To further improve the imaging, a virus with a fluorescent protein could be designed that has its excitation and emission wavelengths that are very narrow or even more separated from the other proteins. Otherwise also a mouse strain crossbreed could be designed with another fluorescent protein following the before-stated criteria.

5.7 Ethical discussion

To justify the use of animals for research purposes an ethical approval is necessary, the importance of the gain needs to be clear and the welfare of the animals must always be respected. The three R's of Replacement, Reduction, and Refinement can act as guiding principles. For this project, the use of animals is necessary and can't be replaced by organoids or cell cultures for the reason that the brain is too complex with all its intercellular interactions. Also, the neurons need to be investigated in the context of a whole network that contains about 10000 different types of cells. So, if for this project a model other than an animal would be used, the results would very likely not be meaningful or applicable to humans. However, the number of mice involved can be minimized. As mentioned before, for the purpose of this project, to detect the loss of the NeuN protein in OLM α 2 cells and the identification for the optimal injection amount can be done by using few animals. Although, too few animals would also not be the way to go, since then the results could have been made by chance. Lastly, it is important to minimize animal suffering and improve their welfare. In

this project the focus laid on effective analgesia and anesthesia protocol. Also, careful post-operational monitoring is important. One animal had lost a stitch after the virus injection and had to be anesthetized for a new one. This is a stressful procedure and therefore the post-operational care could be refined.

5.8 Outlook on future projects

After finding the optimal parameters for the virus injection, the next step would be the downregulation of the *Chrna2* containing nicotinic receptors of OLM cells. Previously it has been shown that fear learning is impaired after genetic deletion of *Chrna2* nAChRs (Lotfipour et al. 2017). As mentioned before, these receptors seem to modulate the hippocampus in response to stress. Consistent with this, after the knockout of *Chrna2* nAChR in OLM cells, a shock-paired tone diminished the freezing of mice, and also in a forced swimming test, the time the mice spent immobile was lower. The authors concluded that by decreasing acetylcholine signaling in these receptors, also OLM cells decreased their activity and imbalanced the hippocampus (Mineur et al. 2020).

In an animal model of Alzheimer's disease, dysfunction in OLM cell activity and memory deficits were recently associated (Schmid et al. 2016). This corresponds to the general idea, that OLM cells play a major role in memory formation in the hippocampus. Mutations in the *Chrna2* gene are also linked to epilepsy (Aridon et al. 2006) and benign familial infantile seizures (Trivisano et al. 2015) in humans.

5.9 Conclusion

In this study, first, the methods that provided the best results for the analysis were defined. The procedure to create the sections using the vibratome was advantageous compared to the cryostat because there perfect sections could be ensured every time. Also, the vibratome allowed to cut thicker sections at 60 μm , which means more whole cells can be found in one section. Then the immunohistochemical protocols were examined and protocol 2, described in the methods section, was selected since it could ensure clear staining with fewer products and steps compared to protocol 1. Furthermore, the secondary antibodies were all produced in the same animal as the blocking solution, which lowers the probability of non-specific binding.

Then, the expression of the NeuN protein could be confirmed in 84 % of the OLM α 2 cells, which was lowered to 49 % in the cells infected by the virus. This means, that the knockout was successful and therefore the Cas9 protein is functional in this setup. The optimal virus volume was 500 nl, as the virus was able to infect a wide area in the ventral hippocampus, around 2 mm² at its widest point along the transversal plane. The study presented here was aimed to improve the knowledge and understanding of neuronal networks that regulate memory formation in health and disease.

6. Summary

In the brain, the hippocampus plays an important role in memory formation and it is closely tied to emotion. The control of the input and distribution of excitatory signaling in neuronal circuits is essential and regulators like the oriens lacosum moleculare cells are therefore crucial. A genetically defined population are the oriens lacosum moleculare cells that express an $\alpha 2$ subunit in nicotinic acetylcholine receptors. To investigate their role in mice, this subunit can be downregulated and observations of the resulting effects can be made.

In this pilot study, the neuronal nuclear protein was targeted instead of the *Chrna2*, to find the optimal parameters and validate the methods. This protein is abundantly expressed in most neurons and therefore, a good control of downregulation. To lower the protein levels, a Clustered Regularly Interspaced Short Palindromic Repeats/Cas9 system was used to knockout the *Rbfox3* gene corresponding to the neuronal nuclear protein. A mouse strain crossbred expressed the Cas9 protein in the cells expressing the $\alpha 2$ subunit and the small guiding RNA was delivered by an adeno-associated virus. To observe the virus, it also expressed the mCherry fluorescent protein. After the injection, the mouse brains were sectioned and stained immunohistochemically to visualize the oriens lacosum moleculare cells with the $\alpha 2$ subunit and the neuronal nuclear protein. Using a widefield and confocal microscope, the sections were imaged and analyzed.

In this study, the methods that provided the best results for the analysis were defined, as well as the optimal injection volume of the virus for the target area. The neuronal nuclear protein expression could be confirmed in 84 % of the oriens lacosum moleculare cells with the $\alpha 2$ subunit, which was lowered to 49 % in the cells infected by the virus. This means, that the knockout was successful and therefore the Cas9 protein is functional in this setup.

Specifically, these findings can be used in future behavioral studies when downregulating the $\alpha 2$ subunit in nicotinic acetylcholine receptors to address the effect of the inhibition of oriens lacosum moleculare cells in an anxiogenic context.

7. Zusammenfassung

Im Gehirn spielt der Hippocampus eine wichtige Rolle beim Gedächtnis und er ist eng mit Emotionen verbunden. Die Kontrolle der eingehenden exzitatorischen Signale und deren Verteilung ist in neuronalen Schaltkreisen essentiell, und Regulatoren wie die oriens lacosum moleculare-Zellen sind daher wesentlich. Eine genetisch definierte Population sind die oriens lacosum moleculare-Zellen, die eine $\alpha 2$ Untereinheit in nikotinischen Acetylcholinrezeptoren exprimieren. Um ihre Rolle in Mäusen zu untersuchen, kann die $\alpha 2$ -Untereinheit herunterreguliert und die daraus resultierenden Effekte beobachtet werden.

In dieser Pilotstudie wurde das NeuN Protein anstelle der $\alpha 2$ -Untereinheit anvisiert, um die Methoden zu validieren. Das NeuN Protein wird in den meisten Neuronen abundant exprimiert und ist daher eine gute Kontrolle für die Herunterregulierung. Um die Proteinkonzentrationen zu senken, wurde ein „Clustered Regularly Interspaced Short Palindromic Repeats“/Cas9-System verwendet, das das Rbfox3-Gen ausschaltet, welches für das NeuN Protein kodiert. Eine Mausstammkreuzung exprimiert das Cas9-Protein in den Zellen, die die $\alpha 2$ -Untereinheit exprimieren. Eine „small guiding“ RNA wurde von einem adeno-assoziiertem Virus geliefert. Um das Virus zu beobachten, exprimiert es auch das mCherry-Fluoreszenzprotein. Nach der Injektion wurden die Mäusegehirne geschnitten und immunhistochemisch gefärbt, um die oriens lacosum moleculare-Zellen mit der $\alpha 2$ Untereinheit und das neuronale Nuclearprotein zu visualisieren. Mit Hilfe eines Weitfeld- und eines konfokalen Mikroskops wurden die Schnitte untersucht und ausgewertet.

In dieser Studie wurden die Methoden definiert, die die besten Ergebnisse für die Analyse lieferten, sowie das optimale Injektionsvolumen des Virus. Die NeuN Proteinexpression konnte in 84 % der oriens lacosum moleculare-Zellen mit der $\alpha 2$ Untereinheit nachgewiesen werden. In den Zellen, die mit dem Virus infiziert waren, wurde das Level auf 49 % gesenkt. Folglich war der Knockout erfolgreich und das Cas9-Protein ist in diesem System funktional.

Konkret können diese Resultate in zukünftigen Verhaltensstudien verwendet werden, wenn die $\alpha 2$ Untereinheit in nikotinischen Acetylcholinrezeptoren herunterreguliert werden soll, um die Wirkung der Hemmung von oriens lacosum moleculare-Zellen in einem anxiogenen Kontext zu untersuchen.

8. Keywords and abbreviations

AAV = adeno-associated virus

CA1 = cornu ammonis area 1

Ca²⁺ = Calcium²⁺

CA3 = cornu ammonis area 3

Chrna2 = neuronal acetylcholine receptor subunit alpha-2

CRISPR = Clustered Regularly Interspaced Short Palindromic Repeats

DAPI = 4', 6-diamidino-2-fenylindol

EC = entorhinal cortex

EGFP = enhanced green fluorescent protein

GABA = γ -aminobutyric acid

LTP = long-term potentiation

NA = numerical aperture

nAChR = nicotinic acetylcholine receptors

NeuN = neuronal nuclear protein

OLM = oriens lacunosum moleculare

OLM α 2 = oriens lacunosum moleculare cells expressing the neuronal acetylcholine receptor subunit alpha-2 in nicotinic acetylcholine receptors

PBS = phosphate buffered saline

pre-mRNA = precursor messenger RNA

sgRNA = small guide RNA

VG = viral genome

9. Contributions

Angelica Thulin designed the study and performed the virus injections. Katharina Ambroz performed the genotyping and the perfusions of all mice.

10. Acknowledgments

First and foremost I would like to express my very great appreciation to my supervisors Professor Klas Kullander and Angelica Thulin for taking me in and for giving me the opportunity to do research as a part of the Research group: Formation and Function of Neuronal Circuits at the Department of Neuroscience, Uppsala University, Sweden. I also wish to acknowledge the help provided by my supervisor Dr. Rudolf Moldzio at my home University and thank all three for proofreading my thesis and providing great constructive suggestions to improve the quality, as well as the scientific accuracy. My deepest gratitude goes to Angelica Thulin for introducing me to the topic and promoting my interest in uncovering the mysteries of the hippocampal circuits. Her vision, passion and conscientiousness have deeply inspired me. I also want to thank her, for always being calm and understanding, especially when I made mistakes. Additionally, I had the pleasure of being tutored by Katherina Ambroz, who showed me the robes in the lab and supported me in the beginning with my experiments. I want to thank her for her patience and for always having an open ear. Furthermore, I would like to express my gratitude for Jennifer Vieillard for introducing me to the widefield microscope and Jeremy Adler for showing me my way around the confocal microscope and giving me valuable feedback on how I could improve my imaging. Advice given by Klara Thurner has been a great help when sectioning the brains with the cryostat. I would also like to express my appreciation for the Erasmus+ program committee for supporting my education financially and enabling my stay in Uppsala. My everyday life in the lab was especially enriched by David Smeele and I am very grateful for our conversations, your humor and compassion. I am extending my heartfelt thanks to my parents, Judith and Herbert Amort for their love and encouragement regarding not only my education, but all aspects of my life. Then, I want to express my deepest gratitude to my sister, Julia Amort and my boyfriend, Elias Gruber, for their love, emotional support and help whenever I was struggling. My special thanks are also dedicated to all my coworkers and friends, for the adventures and memories created during this time. It was a great privilege and honor to work and study in this research group and I am extremely grateful for all my experiences here. Lastly, I want to express my deepest thanks to all the people, who have supported me to complete the research work directly or indirectly.

11. References

- Aridon, Paolo, Carla Marini, Chiara Di Resta, Elisa Brillì, Maurizio De Fusco, Fausta Politi, Elena Parrini, et al. 2006. "Increased Sensitivity of the Neuronal Nicotinic Receptor $\alpha 2$ Subunit Causes Familial Epilepsy with Nocturnal Wandering and Ictal Fear." *The American Journal of Human Genetics*. <https://doi.org/10.1086/506459>.
- Alkadhi, Karim A. 2019. "Cellular and Molecular Differences Between Area CA1 and the Dentate Gyrus of the Hippocampus." *Molecular Neurobiology* 56 (9): 6566–80.
- Andersen, Per, Richard Morris, David Amaral, John O'Keefe, Tim Bliss, and Division of Neurophysiology Tim Bliss. 2007. *The Hippocampus Book*. Oxford University Press.
- Cannon, Jason R., and J. Timothy Greenamyre. 2009. "NeuN Is Not a Reliable Marker of Dopamine Neurons in Rat Substantia Nigra." *Neuroscience Letters* 464 (1): 14–17.
- Cong, Le, F. Ann Ran, David Cox, Shuailiang Lin, Robert Barretto, Naomi Habib, Patrick D. Hsu, et al. 2013. "Multiplex Genome Engineering Using CRISPR/Cas Systems." *Science* 339 (6121): 819–23.
- Cortez, Jessica T., Elena Montauti, Eric Shifrut, Jovylyn Gatchalian, Yusi Zhang, Oren Shaked, Yuanming Xu, et al. 2020. "CRISPR Screen in Regulatory T Cells Reveals Modulators of Foxp3." *Nature* 582 (7812): 416–20.
- Daoudal, Gaël, and Dominique Debanne. 2003. "Long-Term Plasticity of Intrinsic Excitability: Learning Rules and Mechanisms." *Learning & Memory* 10 (6): 456–65.
- Davis, Jennifer A., and Thomas J. Gould. 2008. "Associative Learning, the Hippocampus, and Nicotine Addiction." *Current Drug Abuse Reviews* 1 (1): 9–19.
- Doller, H. J., and F. F. Weight. 1982. "Perforant Pathway Activation of Hippocampal CA1 Stratum Pyramidale Neurons: Electrophysiological Evidence for a Direct Pathway." *Brain Research* 237 (1): 1–13.
- Fanselow, Michael S., and Hong-Wei Dong. 2010. "Are the Dorsal and Ventral Hippocampus Functionally Distinct Structures?" *Neuron* 65 (1): 7–19.
- Fornasiero, Eugenio F., Sunit Mandad, Hanna Wildhagen, Mihai Alevra, Burkhard Rammner, Sarva Keihani, Felipe Opazo, et al. 2018. "Precisely Measured Protein Lifetimes in the Mouse Brain Reveal Differences across Tissues and Subcellular Fractions." *Nature Communications* 9 (1): 4230.

- Freund, T. F., and G. Buzsáki. 1996. "Interneurons of the Hippocampus." *Hippocampus* 6 (4): 347–470.
- Gusel'nikova, V. V., and D. E. Korzhevskiy. 2015. "NeuN As a Neuronal Nuclear Antigen and Neuron Differentiation Marker." *Acta Naturae*. <https://doi.org/10.32607/20758251-2015-7-2-42-47>.
- Haam, Juhee, Jingheng Zhou, Guohong Cui, and Jerrel L. Yakel. 2018. "Septal Cholinergic Neurons Gate Hippocampal Output to Entorhinal Cortex via Oriens Lacunosum Moleculare Interneurons." *Proceedings of the National Academy of Sciences of the United States of America* 115 (8): E1886–95.
- Harris, Kenneth D., Hannah Hochgerner, Nathan G. Skene, Lorenza Magno, Linda Katona, Carolina Bengtsson Gonzales, Peter Somogyi, Nicoletta Kessaris, Sten Linnarsson, and Jens Hjerling-Leffler. 2018. "Classes and Continua of Hippocampal CA1 Inhibitory Neurons Revealed by Single-Cell Transcriptomics." *PLoS Biology* 16 (6): e2006387.
- Hasselmo, Michael E., Clara Bodelón, and Bradley P. Wyble. 2002. "A Proposed Function for Hippocampal Theta Rhythm: Separate Phases of Encoding and Retrieval Enhance Reversal of Prior Learning." *Neural Computation* 14 (4): 793–817.
- Hilscher, Markus M., Richardson N. Leão, Steven J. Edwards, Katarina E. Leão, and Klas Kullander. 2017. "Chrna2-Martinotti Cells Synchronize Layer 5 Type A Pyramidal Cells via Rebound Excitation." *PLoS Biology* 15 (2): e2001392.
- Ishii, Katsuyoshi, Jamie K. Wong, and Katumi Sumikawa. 2005. "Comparison of $\alpha 2$ Nicotinic Acetylcholine Receptor Subunit mRNA Expression in the Central Nervous System of Rats and Mice." *The Journal of Comparative Neurology*. <https://doi.org/10.1002/cne.20762>.
- Jia, Yousheng, Yoshihiko Yamazaki, Sakura Nakauchi, and Katumi Sumikawa. 2009. "Alpha2 Nicotine Receptors Function as a Molecular Switch to Continuously Excite a Subset of Interneurons in Rat Hippocampal Circuits." *The European Journal of Neuroscience* 29 (8): 1588–1603.
- Kenney, Justin W., Jonathan D. Raybuck, and Thomas J. Gould. 2012. "Nicotinic Receptors in the Dorsal and Ventral Hippocampus Differentially Modulate Contextual Fear Conditioning." *Hippocampus* 22 (8): 1681–90.

- Kim, Kee K., Robert S. Adelstein, and Sachiyo Kawamoto. 2009. "Identification of Neuronal Nuclei (NeuN) as Fox-3, a New Member of the Fox-1 Gene Family of Splicing Factors." *The Journal of Biological Chemistry* 284 (45): 31052–61.
- Kim, Kee K., Joseph Nam, Yoh-Suke Mukoyama, and Sachiyo Kawamoto. 2013. "Rbfox3-Regulated Alternative Splicing of Numb Promotes Neuronal Differentiation during Development." *The Journal of Cell Biology* 200 (4): 443–58.
- Klausberger, Thomas, and Peter Somogyi. 2008. "Neuronal Diversity and Temporal Dynamics: The Unity of Hippocampal Circuit Operations." *Science* 321 (5885): 53–57.
- Kloosterman, Fabian, Theo Van Haeften, Menno P. Witter, and Fernando H. Lopes Da Silva. 2003. "Electrophysiological Characterization of Interlaminar Entorhinal Connections: An Essential Link for Re-Entrance in the Hippocampal-Entorhinal System." *The European Journal of Neuroscience* 18 (11): 3037–52.
- Knowles, W. D. 1992. "Normal Anatomy and Neurophysiology of the Hippocampal Formation." *Journal of Clinical Neurophysiology: Official Publication of the American Electroencephalographic Society* 9 (2): 252–63.
- Lawrence, J. Josh, Jeffrey M. Statland, Zachary M. Grinspan, and Chris J. McBain. 2006. "Cell Type-Specific Dependence of Muscarinic Signalling in Mouse Hippocampal Stratum Oriens Interneurons." *The Journal of Physiology* 570 (Pt 3): 595–610.
- Leão, Richardson N., Sanja Mikulovic, Katarina E. Leão, Hermany Munguba, Henrik Gezelius, Anders Enjin, Kalicharan Patra, et al. 2012. "OLM Interneurons Differentially Modulate CA3 and Entorhinal Inputs to Hippocampal CA1 Neurons." *Nature Neuroscience* 15 (11): 1524–30.
- Lind, Daniela, Sebastian Franken, Joachim Kappler, Jakob Jankowski, and Karl Schilling. 2005. "Characterization of the Neuronal Marker NeuN as a Multiply Phosphorylated Antigen with Discrete Subcellular Localization." *Journal of Neuroscience Research* 79 (3): 295–302.
- Lisman, J. E., and N. A. Otmakhova. 2001. "Storage, Recall, and Novelty Detection of Sequences by the Hippocampus: Elaborating on the SOCRATIC Model to Account for Normal and Aberrant Effects of Dopamine." *Hippocampus* 11 (5): 551–68.
- Lotfipour, Shahrddad, Celina Mojica, Sakura Nakauchi, Marcela Lipovsek, Sarah Silverstein, Jesse Cushman, James Tirtorahardjo, et al. 2017. "α2* Nicotinic Acetylcholine Receptors Influence

- Hippocampus-Dependent Learning and Memory in Adolescent Mice.” *Learning & Memory* 24 (6): 231–44.
- Lovett-Barron, Matthew, Patrick Kaifosh, Mazen A. Kheirbek, Nathan Danielson, Jeffrey D. Zaremba, Thomas R. Reardon, Gergely F. Turi, René Hen, Boris V. Zemelman, and Attila Losonczy. 2014. “Dendritic Inhibition in the Hippocampus Supports Fear Learning.” *Science* 343 (6173): 857–63.
- Lynch, M. A. 2004. “Long-Term Potentiation and Memory.” *Physiological Reviews* 84 (1): 87–136.
- Maccaferri, G., and C. J. McBain. 1995. “Passive Propagation of LTD to Stratum Oriens-Alveus Inhibitory Neurons Modulates the Temporoammonic Input to the Hippocampal CA1 Region.” *Neuron* 15 (1): 137–45.
- Madisen, Linda, Theresa A. Zwingman, Susan M. Sunkin, Seung Wook Oh, Hatim A. Zariwala, Hong Gu, Lydia L. Ng, et al. 2010. “A Robust and High-Throughput Cre Reporting and Characterization System for the Whole Mouse Brain.” *Nature Neuroscience* 13 (1): 133–40.
- Maxeiner, Stephan, Alexander Glassmann, Hung-Teh Kao, and Karl Schilling. 2014. “The Molecular Basis of the Specificity and Cross-Reactivity of the NeuN Epitope of the Neuron-Specific Splicing Regulator, Rbfox3.” *Histochemistry and Cell Biology* 141 (1): 43–55.
- McPhail, Lowell T., Christopher B. McBride, John McGraw, John D. Steeves, and Wolfram Tetzlaff. 2004. “Axotomy Abolishes NeuN Expression in Facial but Not Rubrospinal Neurons.” *Experimental Neurology*. <https://doi.org/10.1016/j.expneurol.2003.10.001>.
- Mikulovic, Sanja, Carlos Ernesto Restrepo, Samer Siwani, Pavol Bauer, Stefano Pupe, Adriano B. L. Tort, Klas Kullander, and Richardson N. Leão. 2018. “Ventral Hippocampal OLM Cells Control Type 2 Theta Oscillations and Response to Predator Odor.” *Nature Communications* 9 (1): 3638.
- Mineur, Yann S., Charlotte Ernsten, Ashraful Islam, Kathrine Lefoli Maibom, and Marina R. Picciotto. 2020. “Hippocampal Knockdown of $\alpha 2$ Nicotinic or M1 Muscarinic Acetylcholine Receptors in C57BL/6J Male Mice Impairs Cued Fear Conditioning.” *Genes, Brain, and Behavior* 19 (6): e12677.
- Mullen, R. J., C. R. Buck, and A. M. Smith. 1992. “NeuN, a Neuronal Specific Nuclear Protein in Vertebrates.” *Development*. <https://doi.org/10.1242/dev.116.1.201>.

- Peng, Can, Yijin Yan, Veronica J. Kim, Staci E. Engle, Jennifer N. Berry, J. Michael McIntosh, Rachael L. Neve, and Ryan M. Drenan. 2019. "Gene Editing Vectors for Studying Nicotinic Acetylcholine Receptors in Cholinergic Transmission." *The European Journal of Neuroscience* 50 (3): 2224–38.
- Platt, Randall J., Sidi Chen, Yang Zhou, Michael J. Yim, Lukasz Swiech, Hannah R. Kempton, James E. Dahlman, et al. 2014. "CRISPR-Cas9 Knockin Mice for Genome Editing and Cancer Modeling." *Cell* 159 (2): 440–55.
- Portiansky, Enrique Leo, Claudio Gustavo Barbeito, Eduardo Juan Gimeno, Gustavo Oscar Zuccolilli, and Rodolfo Gustavo Goya. 2006. "Loss of NeuN Immunoreactivity in Rat Spinal Cord Neurons during Aging." *Experimental Neurology* 202 (2): 519–21.
- Schmid, Lena C., Manuel Mittag, Stefanie Poll, Julia Steffen, Jens Wagner, Hans-Rüdiger Geis, Inna Schwarz, et al. 2016. "Dysfunction of Somatostatin-Positive Interneurons Associated with Memory Deficits in an Alzheimer's Disease Model." *Neuron*. <https://doi.org/10.1016/j.neuron.2016.08.034>.
- Siwani, Samer. 2021. Hippocampal Circuit Dynamics in Learning and Value Processing of Sensory Cues: A Study into the Function of Hippocampal Microcircuits Involving OLM $\alpha 2$ Cells [Dissertation]. Uppsala University.
- Siwani, Samer, Arthur S. C. França, Sanja Mikulovic, Amilcar Reis, Markus M. Hilscher, Steven J. Edwards, Richardson N. Leão, Adriano B. L. Tort, and Klas Kullander. 2018. "OLM $\alpha 2$ Cells Bidirectionally Modulate Learning." *Neuron* 99 (2): 404–12.e3.
- Son, Jong-Hyun, and Ursula H. Winzer-Serhan. 2008. "Expression of Neuronal Nicotinic Acetylcholine Receptor Subunit mRNAs in Rat Hippocampal GABAergic Interneurons." *The Journal of Comparative Neurology* 511 (2): 286–99.
- Strange, Bryan A., Menno P. Witter, Ed S. Lein, and Edvard I. Moser. 2014. "Functional Organization of the Hippocampal Longitudinal Axis." *Nature Reviews. Neuroscience* 15 (10): 655–69.
- Trivisano, Marina, Alessandra Terracciano, Teresa Milano, Simona Cappelletti, Nicola Pietrafusa, Enrico Silvio Bertini, Federico Vigeveno, and Nicola Specchio. 2015. "Mutation of CHRNA2 in a Family with Benign Familial Infantile Seizures: Potential Role of Nicotinic Acetylcholine Receptor in Various Phenotypes of Epilepsy." *Epilepsia*. <https://doi.org/10.1111/epi.12967>.

- Tyan, Leonid, Simon Chamberland, Elise Magnin, Olivier Camiré, Ruggiero Francavilla, Linda Suzanne David, Karl Deisseroth, and Lisa Topolnik. 2014. "Dendritic Inhibition Provided by Interneuron-Specific Cells Controls the Firing Rate and Timing of the Hippocampal Feedback Inhibitory Circuitry." *The Journal of Neuroscience: The Official Journal of the Society for Neuroscience* 34 (13): 4534–47.
- Unal-Cevik, Isin, Münire Kiliç, Yasemin Gürsoy-Ozdemir, Gunfer Gurer, and Turgay Dalkara. 2004. "Loss of NeuN Immunoreactivity after Cerebral Ischemia Does Not Indicate Neuronal Cell Loss: A Cautionary Note." *Brain Research* 1015 (1-2): 169–74.
- Whittington, M. A., R. D. Traub, and J. G. Jefferys. 1995. "Synchronized Oscillations in Interneuron Networks Driven by Metabotropic Glutamate Receptor Activation." *Nature* 373 (6515): 612–15.

12. Appendix

12.1. Mouse strains

The animal experiments used in this study were approved by the local Swedish ethical committee (Dnr C63/16). All animals were kept, bred, and housed according to the regulation and guidelines of Jordbruksverket with the ethical permission (Dnr 5.8.18-11551/2019).

12.1.1 Chrna2-cre/tdTomato, a first transgenic mouse strain is expressing the cre recombinase under the control of the Chrna2 promoter (Leão et al. 2012). These mice are crossed with a mouse strain that expresses a genetic construct for the expression of the fluorescent tdTomato protein in a cre-dependent manner (JAX stock #007914; Madisen et al. 2010). These transgenic mice, therefore, expressed the tdTomato protein only in Chrna2 positive cells, where the cre recombinase is present. This strain was used to identify the OLM α 2 cells and to optimize the methods like the sectioning and the immunohistochemistry. Two female mice were used, which were sacrificed when eight weeks old.

12.1.2 Chrna2-cre/Cas9EGFP, a first transgenic mouse strain is expressing the cre recombinase under the control of the Chrna2 promoter (Leão et al. 2012). These mice are crossed with a mouse strain that expresses a genetic construct for the expression of Cas9 and EGFP in a cre-dependent manner (JAX stock #026179, Cortez et al. 2020; Platt et al. 2014). Therefore, these mice can express the Cas9 and EGFP protein only in Chrna2 positive cells, where the cre recombinase is present. The mice were used in this project to observe the spread of the injected virus and the function of Cas9 with the help of the downregulation of the NeuN protein. Four female mice were, two were sacrificed when 36 weeks and the other two when 29 weeks old.

12.1.3 Genotyping

To confirm the genotype of the mouse strains, a biopsy sample from the ear was taken. 50 μ l of Tail Buffer 1 (25 mmol sodium hydroxide, 0.2 mmol EDTA in distilled water) was added and put in the shaking box (Mixing Block MB-102, Bioer, China) for 25 min and 96 degrees at 300 speed. Then, 50 μ l of Tail Buffer 2 (40 mmol TRIS hydrochloride, pH 8 in distilled

water) was added to the samples. For all mice, we could validate the Chrna2-cre expression with the primers with the sequences of GACAGCCATTTTCTCGCTTC (forward) and AGGCAAATTTTGGTGTACGG (reverse). The tdTomato mutants were confirmed with the primers with the sequences of CTGTTCTGTACGGCATGG (forward) and GGCATTAAGCAGCGTATCC (reverse) and the wildtypes were excluded by using the primers with the sequences AAGGGAGCTGCAGTGGAGTA (forward) and CCGAAAATCTGTGGGAAGTC (reverse). And finally, the EGFP was validated with the use of the primers with the sequences of GACGTAAACGGCCACAAGTTC (forward) and CTTCTCGTTGGGGTCTTTGCT (reverse) and the wildtypes were excluded by using the primers with the sequences AAGGGAGCTGCAGTGGAGTA (forward) and CCGAAAATCTGTGGGAAGTC (reverse). For the PCR, to 1 μ l of each sample was added 2.5 μ l KAPA Buffer (Sigma-Aldrich Corp., USA), 0.5 μ l Deoxynucleotide (VWR, USA), 0.5 μ l KAPA Taq Polymerase (Sigma-Aldrich Corp., USA) and 1 μ l of each primer. The rest to 25 μ l was then filled up with MilliQ water. The PCR programs were run on a thermal cycler (S1000 Thermal Cycler, Bio-Rad, USA) with the programs stated in Table 6. An agarose gel was used (2 % agarose (VWR, USA) in 1 \times TAE-buffer (VWR, USA)) with ethidium bromide (Sigma-Aldrich Corp., USA) at 2 drops (~100 μ l) per 150 ml. The samples were then run in an electrophoresis at 165 V with 250 mA and 50 W for 30 min (power supply: Consort EV243 power supply, Sigma-Aldrich Corp., USA). The samples were evaluated with a transilluminator (Tehtum Lab Ab, Sweden).

	EGFP (wildtype)		Chrna2-cre		EGFP (transgenic)		TdTomato	
order	Temperature	Time	Temperature	Time	Temperature	Time	Temperature	Time
1	94 °C	2 min	95 °C	3 min	94 °C	2 min	95 °C	3 min
2	94 °C	30 sec	95 °C	30 sec	94 °C	50 sec	95 °C	30 sec
3	65 °C	30 sec	55 °C	30 sec	65 °C	45 sec	61 °C	40 sec
4	68 °C	30 sec	72 °C	40 sec	72 °C	45 sec	72 °C	1 min
5	Repeat 2-4 for 9 times		Repeat 2-4 for 30 times		Repeat 2-4 for 35 times		Repeat 2-4 for 33 times	
6	94 °C	30 sec	72 °C	6 min	72 °C	2 min	72 °C	5 min
7	60 °C	30 sec	10 °C	forever	10 °C	forever	10 °C	forever
8	72 °C	30 sec						
9	Repeat 6-8 for 27 times							
10	72 °C	5 min						

Table 6: Programs on the Thermo Cycler for the Genotyping of the mouse strains.

12.2. Virus

12.2.1 Virus production

An AAV was used, which delivered sgRNA to confirm the function of Cas9 when targeting the Rbfox3 gene (encodes the NeuN protein). The plasmid pFB-U6-sgNeuN-gRNA-hSyn-mCherry-WPRE-SV40pA (Addgene plasmid # 128346; <http://n2t.net/addgene:128346>; RRID:Addgene_128346) was a gift from Ryan Drenan (Peng et al. 2019). Based on this plasmid AAV2/1 were produced and quantified by Charité Viral Core Facility, Germany, according to Addgene standard protocols. Quantifications were performed by quantitative PCR of the VG and reached a titer of 2.70×10^{12} VG/ml. The used AAV has two genes deleted, the E1 and E3, and is, therefore, replication-incompetent.

12.2.2 Virus injection: mice C, D, E, F

The mice were injected unilaterally with the virus intracerebrally during anesthesia using isoflurane (2-2.5 % in breathing air, Isofluran Baxter, Apoteket, Sweden). The animals were also given the eye gel carbomer (2.4 mg/g, Oftagel, Santen, Japan). They were provided with

bupivacain (2 mg/kg subcutan, Marcain, Aspen Australia, Australia) and karprofen (5 mg/kg intraperitoneal, Norocarp, Apoteket, Sweden) as local and systemic analgesia during the procedure and buprenorfin (0.1 mg/kg intraperitoneal, Vetergesic, Ceva, France) during awakening. The virus was injected unilaterally into the right side at the following coordinates: AP: -3.2 ML: -3.5 AP: -4.4. The injection rate was at 100 nl/min and the needle was left in position for 5 minutes before the withdrawal. Two mice were injected with a volume of 500 nl, one with 250 nl, and one with 750 nl.

12.3. Perfusion

To prepare the tissue for immunohistochemistry, the brains were first fixed by transcardial perfusions. The two *Chrna2-cre*/tdTomato mice were sacrificed and perfused at eight weeks of age. The perfusion for mouse D was performed nine days after injecting the virus and mice C, E, F were perfused after 24 days. The mice were anesthetized with injections of a mix of ketamin (75 mg/kg intraperitoneal, Ketalar, Pfizer, Sweden) and medetomidin (1 mg/kg intraperitoneal, Domitor, OrionPharma, Sweden). The animals were then perfused transcardially with 1× PBS followed by 4 % formaldehyde in 1× PBS. The brains of mice A and D were placed in 4 % formaldehyde overnight. Then the medium was changed to 1× PBS. The brain of mouse B was also placed in 4 % formaldehyde overnight and then changed to 30 % sucrose in PBS to prepare it for freezing and protect it. The brains of the mice C, E, and F were incubated for 36 h in 4 % formaldehyde then washed 2× for 5 min in 1× PBS, and then placed in 1× PBS until sectioning.